

**SIMULATING GALACTIC WHITE DWARF BINARY FOREGROUNDS FOR
MULTI-SOURCE GRAVITATIONAL WAVE DETECTION WITH LISA**

By

Neel Nilesh Panchal

Thesis Project
Submitted in Partial Fulfillment of the
Requirements for the Degree of

MASTER OF SCIENCE IN PHYSICS
Northwestern University

May 2025

Prof. Shane L Larson, First Reader

Prof. Andrew Geraci, Second Reader

ABSTRACT

The upcoming Laser Interferometer Space Antenna (LISA) mission will open a new observational window onto gravitational waves emitted by compact binary systems across the universe. To realize LISA’s full scientific potential, robust simulations of gravitational wave sources and their galactic distributions are essential. This thesis presents a detailed study of gravitational wave foreground modeling for compact binary populations, leveraging COSMIC—a population synthesis code—and COGSWORTH—a galactic embedding framework that models binary systems within realistic Milky Way-like structures, combined with LEGWORK, a gravitational wave analysis toolkit tailored for LISA sensitivity studies.

Galaxy populations of double white dwarf binaries were generated through COSMIC, spatially embedded within galactic potentials using COGSWORTH, and analyzed for their gravitational wave emission profiles. Special attention was given to modeling the unresolved stochastic foreground, known as the confusion noise, produced by overlapping sources. Using the Cornish et al. (2019) analytic framework, both bounded and unbounded parameter fitting were performed to characterize the spectral structure of the confusion background and assess its sensitivity to population properties.

Results demonstrate that while the spectral shape of the foreground remains stable across different galactic populations under constrained modeling, the total gravitational wave amplitude varies significantly. These findings emphasize the importance of population-specific calibration for future LISA observations. This study integrates data-driven simulation with theoretical modeling to refine gravitational wave forecasting, advancing preparation for LISA’s mission to explore compact binaries and the dynamic history of galaxies in the multi-messenger era.

ACKNOWLEDGEMENTS

This thesis is a culmination of not only months of research and countless hours of dedication and hard work but also the unwavering support, guidance, and encouragement I have received along the way.

First and foremost, I would like to express my deepest gratitude to Professor Shane L. Larson, whose mentorship has been instrumental in shaping this work. His passion for gravitational wave research has been a guiding light throughout this journey. His patience, wisdom, and ability to distill complexity into clarity have shaped not only this work but also my approach to science. His mentorship has been a privilege, and I could not have asked for a better guide through the cosmos.

To my parents, Nilesh D. Panchal and Sapna N. Panchal, whose love and sacrifices have built the foundation upon which I stand, I owe you everything. I am also grateful to my sister, Tisha, whose encouragement and joy have always filled me with happiness. Your unwavering faith in me, your boundless encouragement, and your silent strength have been my anchor. No words can fully capture the depth of my gratitude for the years of hard work and dedication you have poured into my dreams, never once asking for anything in return. Every late-night discussion, every word of encouragement, and every sacrifice you have made to support my dreams has not gone unnoticed. This achievement is as much yours as it is mine.

To my friends, who have been my pillars of support through this journey, thank you for the endless conversations, the much-needed distractions, and the gentle (and sometimes not-so-gentle) reminders that I am more than just my research. Your laughter, encouragement, and companionship have made this journey bearable, even in the most stressful times.

Lastly, to anyone who has ever shared words of encouragement, offered a helping hand, or listened when I needed to talk - thank you.

With heartfelt appreciation,

Neel Nilesh Panchal

A great dedication goes here.

TABLE OF CONTENTS

| | |
|---|----|
| Abstract | 2 |
| List of Tables | 8 |
| List of Figures | 9 |
| Chapter 1: Introduction and Motivation | 10 |
| 1.1 Laser Interferometer Space Antenna (LISA) | 11 |
| 1.2 Gravitational Waves | 13 |
| 1.3 White Dwarfs: Evolution, Binaries, and the Milky Way | 16 |
| 1.3.1 White Dwarfs as Stellar Endpoints | 16 |
| 1.3.2 Why White Dwarfs? | 18 |
| 1.3.3 White Dwarf Binaries in the Milky Way | 19 |
| Chapter 2: Methodology and Results | 22 |
| 2.1 Introduction | 22 |
| 2.2 Methodology | 23 |
| 2.2.1 COSMIC | 23 |
| 2.2.2 White Dwarf background from COSMIC | 26 |
| 2.2.3 LEGWORK: Gravitational Wave Signal Modeling | 29 |

| | | |
|---------------------------|--|----|
| 2.2.4 | Cogsworth | 32 |
| 2.2.5 | Fitting Models | 33 |
| 2.2.6 | Schematic overview of the gravitational wave foreground modeling pipeline. | 36 |
| 2.2.7 | Data & Code Availability. | 37 |
| 2.3 | Simulations | 37 |
| 2.3.1 | Quest: High-Performance Computing (HPC) Setup | 38 |
| 2.3.2 | Simulation Overview and Model Variants | 40 |
| 2.3.3 | Simulation Post-processing and Gravitational Wave Calculations | 43 |
| 2.3.4 | Data Management and Workflow Automation | 46 |
| Chapter 3: Results | | 47 |
| 3.1 | Overview of Simulated Galactic Population | 47 |
| 3.2 | Detectable Sources in Simulated Galactic Population | 47 |
| 3.3 | Characteristic Strain vs. Gravitational Wave Frequency | 50 |
| 3.4 | Fitting Galactic Confusion Noise | 53 |
| 3.5 | Galactic Confusion Noise Model (Cornish et al. 2019) Fits | 54 |
| 3.5.1 | Cornish and Robson Model Fits (With Parameter Bounds) | 55 |
| 3.5.2 | Cornish and Robson Model Fits (Without Parameter Bounds) | 59 |
| 3.6 | Parameter Variation and Analysis | 62 |
| 3.6.1 | Amplitude A : Total Foreground Power | 62 |
| 3.6.2 | Spectral Slope α : High-Frequency Suppression | 63 |
| 3.6.3 | Modulation Amplitude β : Population Irregularity | 63 |
| 3.6.4 | Modulation Frequency κ : Harmonic Bandwidth | 65 |

| | | |
|---|--|----|
| 3.6.5 | Sharpness γ : Confusion Turnover Strength | 65 |
| 3.6.6 | Knee Frequency f_k : Transition Location | 66 |
| 3.7 | Summary of Chapter 3 | 67 |
| Chapter 4: Discussion | | 68 |
| 4.1 | Introduction | 68 |
| 4.2 | How Stable is the Confusion Foreground Across Populations? | 68 |
| 4.3 | What Does the Amplitude Variation Tell Us About Galactic Binaries? | 68 |
| 4.4 | Can Spectral Features Be Reliably Modeled Without Constraints? | 69 |
| 4.5 | Implications for LISA and Future Observations | 69 |
| 4.6 | Limitations of the Current Approach | 69 |
| 4.7 | Chapter Summary | 70 |
| Chapter 5: Conclusion and Future | | 71 |
| 5.1 | Conclusion | 71 |
| 5.2 | Future | 72 |
| 5.3 | Final Note | 73 |
| References | | 76 |

LIST OF TABLES

| | | |
|-----|---|----|
| 2.1 | Parameters of Cornish et al. 2019 | 35 |
| 2.2 | Summary of COGSWORTH simulations used in this study, categorized by <code>kstar</code> type, white dwarf composition, and progenitor metallicity. | 42 |
| 3.1 | Overview of 8 galaxy populations | 48 |
| 3.2 | Cornish and Robson Parameters with Bounds on all eight galaxy populations. | 57 |
| 3.3 | Cornish and Robson Model's Parameters without Bounds on all eight galaxy populations. | 60 |

LIST OF FIGURES

| | | |
|------|---|----|
| 1.1 | Orbital Configuration and Interferometric Structure of LISA[4] | 11 |
| 1.2 | The Spectrum of Gravitational Waves [6]. | 13 |
| 2.1 | Schematic overview of the gravitational wave foreground modeling pipeline. External libraries such as COSMIC, Cogsworth, and LEGWORK were integrated to simulate binary evolution, embed galaxy populations, and compute unresolved background signals. | 37 |
| 3.1 | LISA sensitivity plots showing unresolved sources ($SNR > 7$) for each galaxy. | 49 |
| 3.2 | Strain vs. Gravitational Wave Frequency for each galaxy. | 52 |
| 3.3 | Cornish and Robson Model Fitting with Parameter Bounds. | 58 |
| 3.4 | Cornish and Robson Model Fitting without Parameter Bounds. | 61 |
| 3.5 | Distribution of Amplitude A values across individual populations within the galaxies. | 63 |
| 3.6 | Distribution of α values across individual populations within the galaxies. | 64 |
| 3.7 | Distribution of β values across individual populations within the galaxies. | 64 |
| 3.8 | Distribution of κ values across individual populations within the galaxies. | 65 |
| 3.9 | Distribution of γ values across individual populations within the galaxies. | 66 |
| 3.10 | Distribution of f_k values across individual populations within the galaxies. | 67 |

CHAPTER 1

INTRODUCTION AND MOTIVATION

For centuries, telescopes have been humankind’s eyes to the cosmos. While the exact origins of the telescope remain uncertain, the first patent was filed in 1608 by Dutch eyeglass maker Hans Lippershey, who designed an instrument capable of magnifying objects three times. The following year, Galileo Galilei improved upon this design, building his telescope without ever having seen one. His modifications allowed for 20 \times magnification, making him the first to turn a telescope skyward. This groundbreaking moment revealed mountains and craters on the Moon, the Milky Way as a vast collection of stars, the rings of Saturn, sunspots, and Jupiter’s four largest moons [1].

As time evolved and with its various methods of observing the space around us, astronomy has relied almost exclusively on electromagnetic (EM) radiation—visible light, X-rays, radio waves, and infrared—to decode the universe’s mysteries. Even as technology advanced, every observation was fundamentally limited to what light could reveal. But what if there was more to the cosmos than what could be seen?

Imagine a species that only perceives the world through sight. They could learn a great deal from light alone, but their understanding would be inherently incomplete. Then, one day, they develop the ability to hear—opening an entirely new way of sensing reality. This is precisely what happened in 2015 when the Laser Interferometer Gravitational-Wave Observatory (LIGO) detected gravitational waves for the first time [2].

Unlike light, gravitational waves (GWs) are ripples in spacetime itself—created by some of the most cataclysmic events in the universe, such as colliding black holes, neutron star mergers, and possibly even echoes from the Big Bang[3]. Unlike EM waves, which can be absorbed, scattered, or bent, gravitational waves travel unimpeded through the cosmos, carrying pristine information about their sources.

Ground-based detectors like LIGO have opened this new window, allowing us to ”hear” the

universe in a way never before possible. However, LIGO is sensitive only to high-frequency gravitational waves from relatively small black holes and neutron stars. To truly explore the full spectrum of gravitational waves, we need an observatory in space, free from Earth's seismic noise and capable of detecting long-wavelength gravitational waves from supermassive black holes, binary white dwarfs, and relic waves from the early universe.

This is where the Laser Interferometer Space Antenna (LISA) comes in. As the first space-based gravitational wave observatory, LISA will extend our reach into the cosmos, revealing unseen astrophysical processes that have shaped galaxies, black holes, and the very structure of spacetime itself.

1.1 Laser Interferometer Space Antenna (LISA)

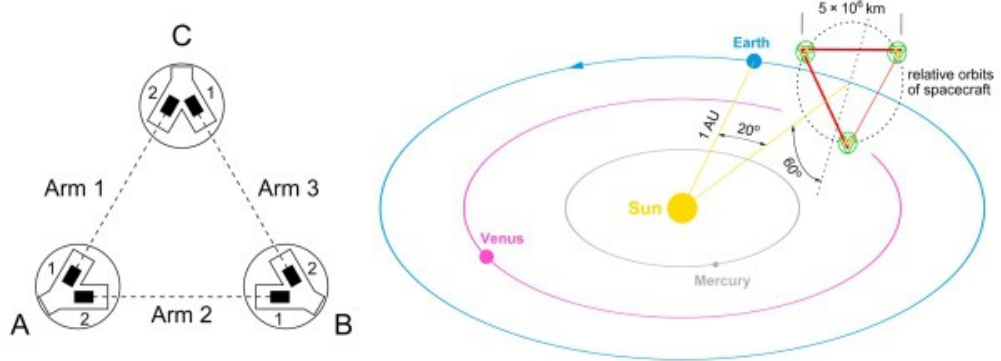


Figure 1.1: Orbital Configuration and Interferometric Structure of LISA[4].

The Laser Interferometer Space Antenna (LISA) is the first planned space-based gravitational wave observatory, designed to detect low-frequency gravitational waves that are inaccessible to ground-based detectors like LIGO and Virgo. Led by the European Space Agency (ESA) with support from NASA, LISA is scheduled for launch in the mid-2030s. It will operate as a triangular interferometer with three spacecraft orbiting the Sun in a precise formation.

LISA measures precise, gravitationally-calibrated absolute luminosity distances to high redshift, with the potential of contributing uniquely to the measurement of the Hubble constant and dark energy [5].

Unlike ground-based detectors, which are constrained by seismic noise and limited arm lengths, LISA will have arms spanning 2.5 million kilometers, allowing it to detect gravitational waves in the millihertz (mHz) range. This makes LISA particularly well-suited for observing compact binary systems, such as White Dwarf binaries, which continuously emit low-frequency gravitational waves throughout their orbital evolution.

LISA's three spacecraft will be arranged in an equilateral triangle, each separated by millions of kilometers and trailing Earth in its orbit around the Sun. These spacecraft will exchange laser beams, forming an ultra-precise interferometer capable of measuring minuscule changes in distance caused by passing gravitational waves. As a wave propagates through the detector, it distorts spacetime, causing slight variations in the lengths of LISA's arms. These changes introduce phase shifts in the laser beams, which LISA measures to extract gravitational wave signals. The fundamental principle governing this detection is:

$$\Delta\phi = \frac{2\pi}{\lambda} hL \quad (1.1)$$

Where $\Delta\phi$ is the phase shift in the laser light, λ is the laser wavelength (1 μm), h is the gravitational wave strain, L is LISA's arm length (2.5 million km). The extreme precision of LISA allows it to detect minor distance fluctuations compared to the width of an atomic nucleus over millions of kilometers.

By operating in space, LISA avoids seismic interference, atmospheric noise, and thermal fluctuations, which limit ground-based detectors. This enables it to continuously observe long-lived gravitational wave sources, such as compact binary systems of White Dwarfs, extreme mass-ratio inspirals (EMRIs), and supermassive black hole mergers (see Figure 1.2). Among these, White Dwarf binaries serve as one of the most significant gravitational wave sources in the Milky Way. LISA will provide the first large-scale gravitational wave map of these systems.

LISA's ability to detect continuous gravitational waves will offer unprecedented insights into stellar remnants, binary evolution, and galactic structure. It will allow scientists to track orbital

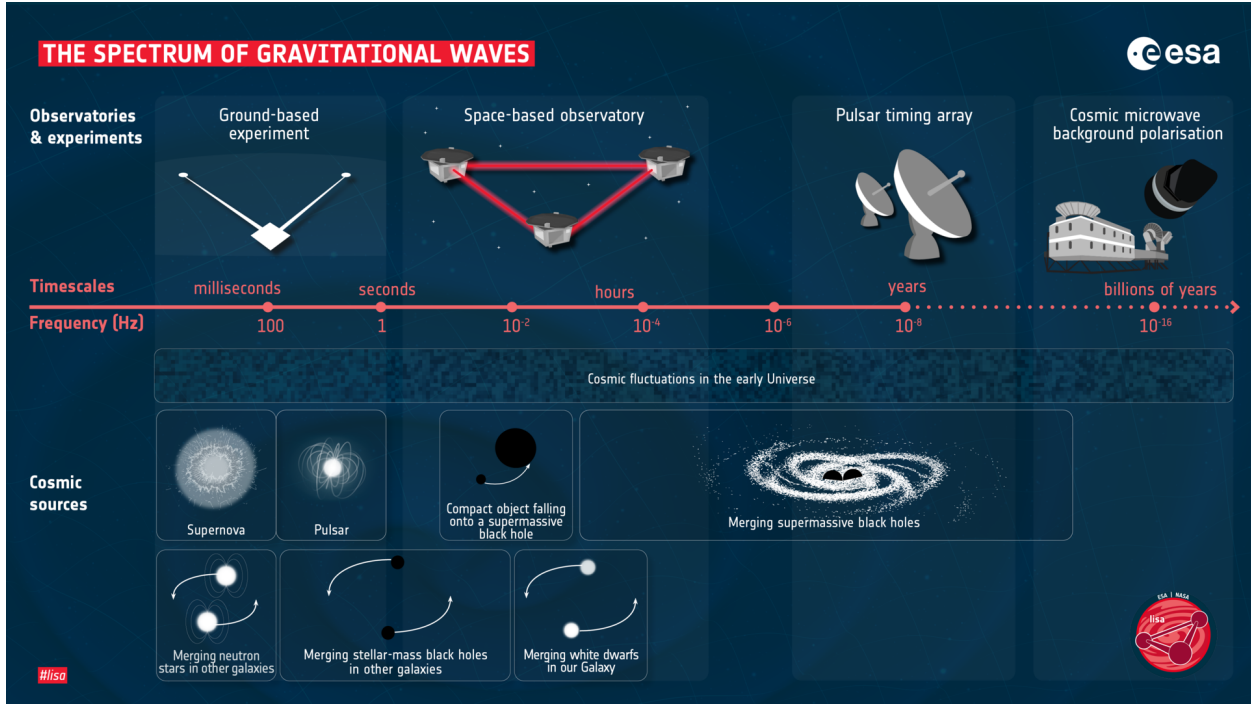


Figure 1.2: The Spectrum of Gravitational Waves [6].

decay in White Dwarf binaries, identifying potential progenitors of Type Ia supernovae and improving our understanding of the Milky Way’s compact object population. As the first mission of its kind, LISA represents a significant leap in gravitational wave astronomy, opening a new window into the universe’s most subtle and long-lived gravitational interactions.

1.2 Gravitational Waves

Gravitational waves (GWs) are ripples in the fabric of spacetime, first predicted by Albert Einstein in 1916 as part of his General Theory of Relativity [7]. Unlike electromagnetic waves, which travel through space as oscillations of electric and magnetic fields, gravitational waves are disturbances in spacetime itself, generated by the acceleration of massive objects. They propagate at the speed of light (c) and carry information about their sources, offering a fundamentally new way to observe the universe.

The first direct detection of gravitational waves was made in 2015 by the Laser Interferometer Gravitational-Wave Observatory (LIGO), confirming Einstein’s century-old prediction and mark-

ing the birth of gravitational wave astronomy [2]. Since then, ground-based detectors such as LIGO, Virgo, and KAGRA have observed multiple events, primarily from merging black holes and neutron stars. However, these detectors are limited to high-frequency gravitational waves (10–1000 Hz) due to their short interferometer arms (~ 4 km) and sensitivity to seismic noise. Many astrophysical sources, such as binary White Dwarfs, extreme mass-ratio inspirals (EMRIs), and supermassive black hole mergers, emit low-frequency gravitational waves (0.1–100 mHz) that ground-based observatories cannot detect. A space-based detector like LISA is required to study these long-lived sources.

The fundamental equation describing gravitational waves is derived from Einstein's field equations [8], which relate the curvature of spacetime ($G_{\mu\nu}$) to the energy-momentum tensor ($T_{\mu\nu}$):

$$G_{\mu\nu} = \frac{8\pi G}{c^4} T_{\mu\nu} \quad (1.2)$$

In the weak-field limit, where perturbations in the metric propagate as waves, the linearized Einstein equations yield the gravitational wave equation[9]:

$$\frac{\partial^2 h_{\mu\nu}}{\partial t^2} - c^2 \nabla^2 h_{\mu\nu} = 0 \quad (1.3)$$

where $h_{\mu\nu}$ represents small perturbations in the metric tensor caused by gravitational waves, $\frac{\partial^2 h_{\mu\nu}}{\partial t^2}$ describes their temporal evolution, and $\nabla^2 h_{\mu\nu}$ represents their spatial propagation. The equation confirms that gravitational waves travel at the speed of light c , similar to electromagnetic waves. Using the d'Alembertian operator (\square), it can be rewritten as:

$$\square h_{\mu\nu} = 0, \quad \text{where} \quad \square = \frac{\partial^2}{\partial t^2} - c^2 \nabla^2. \quad (1.4)$$

This formulation highlights the wave-like nature of gravitational waves, enabling their detection

through interferometric methods.

Quadrupole strain amplitude.

Linearising the Einstein field equations and projecting into the transverse–traceless (TT) gauge gives the quadrupole formula

$$h_{jk}^{\text{TT}}(t) = \frac{2G}{c^4 D} \left[\ddot{Q}_{jk}(t_{\text{ret}}) \right]^{\text{TT}}$$

For a quasi-circular binary, this reduces to two oscillatory polarisations

$$h_+(t) = \frac{1 + \cos^2 i}{2} h_0 \cos \Phi(t), \quad h_\times(t) = \cos i h_0 \sin \Phi(t),$$

with constant scaling amplitude h_0

$$h_0 = \frac{4G\mathcal{M}}{c^2 D} \left(\pi f \frac{G\mathcal{M}}{c^3} \right)^{2/3}, \quad (1.5)$$

where $\mathcal{M} = \mu^{3/5} M^{2/5}$ is the chirp mass, $f = \omega/\pi$ is the gravitational-wave frequency, and D is the luminosity distance [10].

Quadrupole luminosity.

Time-averaging h_{ij}^{TT} over one orbit yields the energy carried by the wave,

$$\left\langle \frac{dE}{dt} \right\rangle = \frac{32}{5} \frac{G^4 \mu^2 M^3}{c^5 a^5}, \quad (1.6)$$

which we use in Chapter 3 to track the orbital decay of white-dwarf binaries.

In a circular binary system, the gravitational wave frequency (f_{GW}) is directly related to the orbital period (P) and the semi-major axis (a) of the orbit. This relationship is given by:

$$f_{GW} = \frac{2}{P} = \frac{1}{\pi} \sqrt{\frac{GM}{a^3}} \quad (1.7)$$

P is the orbital period of the binary system; a is the semi-major axis of the orbit, G is the gravitational constant, and M is the total mass of the binary system. This equation demonstrates that as the binary system loses energy through gravitational wave emission, its orbital period decreases, leading to an increase in gravitational wave frequency over time. This effect, known as chirping, has been observed in LIGO detections of merging black holes and neutron stars, where the inspiral phase accelerates just before the merger. However, White Dwarf binaries emit continuous gravitational waves for millions of years, making them ideal for long-term gravitational wave studies and precise orbital evolution tracking.

The quadrupole formula governs the gravitational wave power emission from a binary system:

$$P_{GW} = \frac{32}{5} \frac{G^4}{c^5} \frac{M_1^2 M_2^2 (M_1 + M_2)}{a^5} \quad (1.8)$$

where P_{GW} is the power radiated via gravitational waves, M_1 and M_2 are the masses of the two binary components, c is the speed of light. This formula highlights why compact binaries, such as White Dwarfs, are significant sources of gravitational waves. Their small separations and high masses result in substantial energy loss via gravitational radiation, making them detectable over extended timescales. The study of these systems with LISA will provide crucial insights into stellar remnants, binary evolution, and galactic gravitational wave populations.

1.3 White Dwarfs: Evolution, Binaries, and the Milky Way

1.3.1 White Dwarfs as Stellar Endpoints

White Dwarfs (WDs) are those compact objects that typically represent the final evolutionary stage of low and intermediate-mass stars ($M \lesssim 8M_\odot$), which constitute the majority of stars in the universe. Such stars undergo a red giant phase when they exhaust their nuclear fuel. This results in them expelling their outer layers into a planetary nebula, leaving behind a compact, dense core. This remnant, supported by electron degeneracy pressure, is a white dwarf - a stellar object unable

to sustain nuclear fusion but remaining luminous due to residual thermal energy[11]. Over time, white dwarfs gradually cool and fade, becoming black dwarfs on cosmic timescales.

The internal composition of a white dwarf depends on the mass and initial metallicity of its progenitor star. The primary types of white dwarfs relevant to astrophysical studies are discussed below.

Helium White Dwarfs (He WDs):

Helium white dwarfs are a type of stellar remnant formed from stars that have undergone significant mass loss, typically from red giants that shed their outer layers[12]. These remnants primarily consist of helium and are often found in binary systems, where they may accrete material from a companion star. Their structure and evolution are closely related to white dwarf physics and the Chandrasekhar limit (approximately $1.4M_{\odot}$), which defines the maximum mass a white dwarf can have before collapsing under its gravity. They are critical objects for studying binary evolution and mass transfer dynamics. They do not undergo helium fusion; instead, they cool and fade over time as they radiate away their remaining thermal energy.

Carbon-Oxygen White Dwarfs (CO WDs):

A carbon-oxygen white dwarf is the final stage of evolution for a low-mass star, where the star's core has collapsed into a dense, compact object composed primarily of carbon and oxygen. This type of white dwarf is the most common end-state for stars that were not massive enough to become supernovae. The carbon and oxygen in the white dwarf's core are the result of nuclear fusion processes that occurred during the star's earlier stages of evolution. Carbon-oxygen white dwarfs can accrete material from a companion star in a binary system, leading to the potential for thermonuclear explosions known as Type Ia supernovae[13]. The extreme density of a carbon-oxygen white dwarf means that the star's gravity can significantly warp the fabric of spacetime, leading to effects like gravitational lensing. They are crucial for understanding supernovae's nucleosynthesis and cosmic distance measurements.

Oxygen-Neon White Dwarfs

An oxygen-neon-magnesium white dwarf is a type of white dwarf star that has a core composed primarily of oxygen and neon, with little to no magnesium. These stars represent the final stage of evolution for low-mass stars, forming after the star has shed its outer layers and the core has collapsed into a dense, degenerate state with initial masses between $8M_{\odot}$ and $10M_{\odot}$. These objects may undergo electron capture-induced core collapse, leading to a Type II supernova or neutron star formation. The study of O-Ne white dwarfs is essential for improving our understanding of stellar remnants, supernovae mechanisms, and the evolution of stars in the higher mass range[14].

1.3.2 Why White Dwarfs?

White dwarfs (WDs) are the final evolutionary stage for the majority of stars with initial masses below $8M_{\odot}$. Comprising over 95% of all stars in the universe, they represent a dominant stellar remnant population within the Milky Way. Characterized by extremely high densities and compact sizes, these objects are supported by electron degeneracy pressure—a quantum mechanical effect that halts further gravitational collapse. Their properties make them ideal for long-term astrophysical studies, particularly in binary systems where their interactions produce measurable astrophysical phenomena. One of the defining characteristics of white dwarfs is their mass-radius relationship, which inversely correlates mass and radius due to the increasing degeneracy pressure with mass. This relationship can be approximated as:

$$R_{WD} \approx 0.013 \left(\frac{M_{WD}}{M_{\odot}} \right)^{-1/3} R_{\odot} \quad (1.9)$$

where R_{WD} is the radius of the white dwarf, M_{WD} is its mass, and R_{\odot} and M_{\odot} are the solar radius and solar mass, respectively[15]. This equation shows that more massive white dwarfs are smaller in size but significantly denser. Typical white dwarfs possess masses around $0.6M_{\odot}$ with radii comparable to Earth's size. White dwarfs are particularly important for gravitational wave astronomy because when found in close binary systems, they become strong, continuous sources

of low-frequency gravitational waves. As these binaries lose energy through gravitational wave emission, their orbits decay, resulting in increasingly stronger signals over time. Moreover, their longevity and stability make them ideal for long-term gravitational wave studies and simulations. The selection of white dwarf binaries for simulations is driven by their: (a) Abundance in the Milky Way, providing a rich dataset for analysis. (b) Predictable gravitational wave signatures due to stable, long-lived orbital dynamics. (c) Potential role as precursors to Type Ia supernovae, providing insights into cosmic events and distance measurements. Thus, simulating Helium (He), Carbon-Oxygen (CO), and Oxygen-Neon (ONe) white dwarf binaries offers a unique opportunity to map their gravitational wave emissions and understand their influence on galactic structure.

1.3.3 White Dwarf Binaries in the Milky Way

The Milky Way is home to billions of white dwarfs, with a significant fraction existing in binary systems. These white dwarf binaries (WDBs) are crucial astrophysical sources, not only for understanding binary evolution but also for their role as prominent emitters of continuous gravitational waves. The prevalence of WDBs across the disk, bulge, and halo of the galaxy contributes to a rich, but complex, gravitational wave landscape. However, their sheer abundance also introduces challenges, particularly when attempting to isolate individual gravitational wave signals. The collective emission of countless unresolved binaries contributes to a stochastic gravitational wave background or confusion noise, complicating detection and analysis. Understanding how these binaries are distributed and how their signals contribute to the gravitational wave foreground is critical for developing effective strategies for simulation and data extraction.

Abundance and Distribution of White Dwarf Binaries

White dwarf binaries are formed through binary evolution pathways, often shaped by common envelope phases and stable mass transfer processes. It is estimated that the Milky Way contains over 10 billion white dwarfs, with a significant fraction existing as compact binaries[16]. These binaries, especially those with orbital periods ranging from minutes to hours, are prolific sources

of continuous gravitational waves within LISA’s sensitive frequency range. The distribution of WDBs is closely linked to the stellar structure of the galaxy. The galactic disk hosts the majority of younger and middle-aged binaries, where recent binary evolution processes have resulted in compact systems with stronger gravitational wave emissions. The bulge contains older, densely packed populations that contribute significantly to the gravitational wave foreground, though individual signals are often weaker due to longer orbital periods. The halo population, while less dense, consists of some of the oldest binaries, remnants of early star formation epochs. These systems typically contribute lower-frequency gravitational wave signals. This widespread distribution not only shapes the Milky Way’s stellar structure but also contributes to a complex gravitational wave landscape that LISA must navigate.

The Challenge of Signal Confusion: Galactic Gravitational Wave Foreground

While the abundance of WDBs makes them valuable for astrophysical studies, it also presents a significant challenge for gravitational wave detection. The sheer number of binaries, particularly in the millihertz frequency range, leads to signal overlap, where multiple gravitational wave signals combine to create a confusion foreground. This stochastic background is especially prominent in the lower-frequency ranges, where unresolved sources produce a persistent, low-level noise that complicates the isolation of individual signals. This confusion noise is expected to dominate LISA’s data at specific frequency ranges, creating a barrier where numerous weak signals overlap, making it difficult to distinguish between individual binaries. The transition from confusion-limited observations to resolvable sources depends on factors such as signal-to-noise ratio, binary distance, and frequency separation. The denser the region, such as the galactic bulge, the greater the challenge in resolving distinct sources. Simulating this foreground is critical for understanding how many signals contribute to the background noise, allowing for better modeling and identification of which frequencies will present the most significant challenges for detection.

How LISA Resolves and Maps the Galactic Binary Population

Despite the challenges posed by the confusion foreground, LISA is designed to isolate and resolve individual gravitational wave signals over time. Its long-baseline interferometry and extended observation periods enhance its ability to distinguish between overlapping signals, particularly for brighter and closer binary systems. As observation time increases, LISA’s frequency resolution improves, enabling it to separate signals that initially appear blended. Techniques such as matched filtering and Bayesian inference will be employed to extract distinct signals from the foreground. By comparing observed waveforms to simulated templates, LISA can identify individual sources based on their orbital characteristics, mass, and distance. This approach will allow LISA to construct a gravitational wave map of the Milky Way, revealing the distribution and characteristics of compact binary systems[17]. Furthermore, cross-referencing resolved WDBs with electromagnetic surveys like Gaia will help validate their positions and improve population models. This integrated approach will provide a more comprehensive view of the galactic structure and binary evolution.

Astrophysical Insights from LISA’s Observations

Through its ability to resolve thousands of WDBs, LISA will provide valuable insights into the formation rates, lifetimes, and evolution of compact binaries. Understanding the distribution of these binaries across the Milky Way will also shed light on the star formation history and the dynamical processes shaping the galaxy. Moreover, identifying potential Type Ia supernova progenitors will enhance our understanding of cosmic distance measurements and contribute to refining cosmological models. Thus, despite the complexities introduced by signal confusion, LISA’s observational strategies and analytical techniques will allow it to extract critical information from the gravitational wave foreground, contributing to a deeper understanding of both binary astrophysics and galactic structure.

CHAPTER 2

METHODOLOGY AND RESULTS

2.1 Introduction

The detection and analysis of gravitational waves (GWs) from compact white dwarf binaries (WDBs) offer critical insights into the structure and evolution of the Milky Way. Simulating these systems provides a deeper understanding of their gravitational wave signatures, informing both current detection strategies and future predictions. This chapter details the methodology adopted for simulating WDB populations using COGSWORTH [18], COSMIC (Compact Object Synthesis and Monte Carlo Investigation Code) framework [19], the development of gravitational wave background models, and the approach taken for modeling and fitting data for further analysis. The simulation process primarily involved two approaches:

1. Fixed Population Models, where initial parameters were constrained to assess specific evolutionary outcomes.
2. Monte Carlo Full Galaxy Simulation, designed to reflect a broader, randomized distribution of binaries, providing a comprehensive view of WDB evolution and gravitational wave emission across the Milky Way.

A key component of the simulation was the construction of the WDBackground model, derived from COGSWORTH outputs. This background represents the cumulative gravitational wave signal from unresolved binaries, where specific parameters such as mass, separation, and orbital frequency directly influence the strength and frequency characteristics of the emitted gravitational waves. Additionally, the gravitational wave strength was analyzed as a function of frequency, considering how distinct binary characteristics manifest in the observable signal landscape.

One of the critical challenges encountered was the need to subtract strong signals - those dominant binary systems whose gravitational wave emissions could obscure or distort the broader signal

distribution. While the exact process for subtraction was iterative, the objective was to minimize confusion noise and enhance the clarity of weaker signals in the dataset. This approach aimed to differentiate between resolvable and non-resolvable sources, ensuring that the background analysis remained robust and accurate.

Another essential aspect of this methodology was the development of unique fitting models. While prior literature provided baseline models for interpreting gravitational wave data, these were adapted and refined to better suit the characteristics observed in the simulation. The goal was to develop new fitting functions that could more accurately describe the relationships between binary parameters and their corresponding gravitational wave signatures. This approach ensured that the thesis contributed novel insights to the field rather than replicating existing models.

The chapter sets the reader up with the apt foundation to comprehend the presentations of simulation results, including key plots and visualizations that capture trends in binary evolution, gravitational wave strength, and frequency distributions. These findings set the stage for further discussion and interpretation, particularly in terms of how the simulations align with current theoretical models and what insights they offer for future gravitational wave studies.

2.2 Methodology

This section details the methodology employed for simulating White Dwarf binaries and their gravitational wave signals. The approach involves generating populations using the COSMIC framework, which COGSWORTH uses to sample the fixed population, analyze gravitational wave backgrounds, and develop fitting models to refine signal characterization.

2.2.1 COSMIC

Overview

COSMIC(Compact Object Synthesis and Monte Carlo Investigation Code) [20] is a publicly available binary population synthesis tool designed for modeling the evolution of stellar binaries, particularly compact object systems such as White Dwarf binaries (WDBs). It is widely used in

astrophysics to simulate the formation, evolution, and final properties of compact binaries, making it an essential framework for understanding their gravitational wave emission. By implementing stellar and binary evolution physics, COSMIC allows for the generation of large-scale populations of WDBs, accounting for critical processes such as:

1. Common-envelope evolution, leading to compact binary formations.
2. Mass transfer episodes, influencing binary separations and stability.
3. Orbital evolution due to gravitational wave emission is crucial for predicting GW signatures detectable by LISA.

COSMIC models the orbital evolution of compact binaries via gravitational wave radiation losses, governed by Peter's equation[21]:

$$\frac{da}{dt} = -\frac{64}{5} \frac{G^3 M_1 M_2 (M_1 + M_2)}{c^5 a^3} \quad (2.1)$$

where a is the semimajor axis of the binary, M_1 & M_2 are the masses of the two objects, G is the gravitational constant, and c is the speed of light. This equation shows how the orbit shrinks over time, leading to stronger GW emission.

COSMIC provides a range of input distributions for initial binary parameters—including mass, orbital separation, and metallicity—to evolve populations of compact binaries over time. The resulting population catalogs contain the properties necessary for modeling gravitational wave strength as a function of frequency, aiding in the construction of WD-Background models for LISA. Two distinct approaches were employed to model WDBs in the Milky Way: the Fixed Population Model, which studies controlled evolutionary pathways, and the Monte Carlo Full Galaxy Model, which provides a more statistically representative population of binaries.

Fixed Population → Monte-Carlo Galaxy

In practice, it is computationally prohibitive to evolve the full $\sim 10^8$ white-dwarf binaries (WDBs) expected in the Milky Way with a detailed binary stellar evolution (BSE) code. We therefore adopt the two-stage strategy recommended in the COGSWORTH documentation: (*i*)construct a moderate-sized **Fixed Population** that faithfully captures the statistical distributions of the present-day WDB phase space, and (*ii*)draw a much larger **Full Galaxy** from that table by Monte-Carlo resampling. The first stage is physics-heavy, the second is statistics-heavy, and the combination delivers both accuracy and scale.

Stage 1 — Fixed Population.

We evolve N_{FP} primordial binaries with COGSWORTH, which passes each system through the complete COSMIC/BSE pipeline (common-envelope, stable mass transfer, magnetic braking, WD cooling) *and* simultaneously integrates its Galactic orbit in a Miyamoto–Nagai potential.

Initial parameters are sampled from the probability-density functions (PDFs):

$$P(a_0) \propto a_0^{-1}, \quad a_{\min} \leq a_0 \leq a_{\max}, \quad (2.2)$$

$$P(M_1) \propto M_1^{-2.35}, \quad M_{\min} \leq M_1 \leq M_{\max}, \quad (2.3)$$

$$P(q) = \text{const.}, \quad 0 \leq q \leq 1, \quad q = \frac{M_2}{M_1}, \quad (2.4)$$

so the evolved catalogue already embodies the observed preference for tight orbits, a Salpeter-like primary-mass function, and a flat mass-ratio spectrum. Because all systems are evolved *individually*, the Fixed Population preserves the *covariances* among orbital period, chirp mass, metallicity, and spatial position—information that would be lost if one drew those quantities independently.

Stage 2 — Full Galaxy (Monte-Carlo resample).

To reach the Galactic birth-rate scale, we perform a Monte-Carlo draw *with replacement* from the Fixed Population, selecting each row with probability proportional to its formation-rate weight

`w_fp`. No new analytic PDFs are introduced at this stage; instead, we amplify the statistically complete seed table to $\mathcal{O}(10^8)$ systems while *retaining* the covariances built in stage 1. Spatial coordinates (x, y, z) assigned during the BSE run are copied unchanged, ensuring that the resampled galaxy respects the same radial and vertical scale lengths.

Why two stages?

Evolving 10^8 binaries with COSMIC/BSE at $\sim 3 - 5$ seconds per system corresponds to $\sim (0.8 - 1.4) \times 10^5$ CPU-hours on a single core [19]. A 5×10^5 -binary Fixed Population therefore costs a manageable $\simeq 10^3$ CPU-hours, after which a Monte-Carlo resample can generate the full Galactic catalogue essentially for free. The Monte-Carlo amplification is computationally trivial but statistically rigorous, because the seed table is already an unbiased draw from Eqs. (2.2)–(2.4). In short, the Fixed Population provides the physics-rich foundation; the Monte-Carlo step scales that foundation to a Milky-Way realisation. All subsequent analysis—LEGWORK strain, SNR masking, PSD binning, and Cornish fitting—is performed on the Full Galaxy but remains grounded in the Fixed Population’s carefully evolved statistical ensemble.

2.2.2 White Dwarf background from COSMIC

The detection of gravitational waves from compact binary populations such as White Dwarf binaries (WDBs) requires an understanding of the gravitational wave background they contribute. The background signal from WDBs in the Milky Way is expected to be one of the dominant astrophysical foregrounds in the LISA sensitivity range. The COSMIC framework was employed to model the population of WDBs, determine their gravitational wave strengths, and construct a realistic representation of the gravitational wave spectrum as a function of frequency.

How Parameters Influence GW Strength

The strength of gravitational wave emission from a binary system is governed by its orbital parameters, component masses, and separation distance. The gravitational wave strain amplitude, which

quantifies the distortion in spacetime due to gravitational radiation, is given by:

$$h \approx \frac{4}{d} \left(\frac{G\mathcal{M}}{c^2} \right)^{\frac{5}{3}} \left(\frac{\pi f_{GW}}{c} \right)^{\frac{2}{3}} \quad (2.5)$$

where h is the gravitational wave strain measured at Earth, d is the distance to the binary system, \mathcal{M} is the chirp mass of the binary (formula shown below), f_{GW} is the gravitational wave frequency, G is the gravitational constant, and c is the speed of light.

The chirp mass of the binary \mathcal{M} [22] or sometimes represented as M_c can be defined as,

$$\mathcal{M} = \frac{(M_1 M_2)^{3/5}}{(M_1 + M_2)^{1/5}} \quad (2.6)$$

The strain amplitude scales inversely with distance ($h \propto 1/d$). It strongly depends on the chirp mass ($h \propto \mathcal{M}^{5/3}$), emphasizing the significance of high-mass binaries in producing stronger gravitational wave signals. The COGSWORTH simulations(using COSMIC for population generation) provided a distribution of WDBs across the Milky Way, enabling the estimation of the expected gravitational wave strain levels from different galactic components such as the disk, bulge, and halo.

GW strength as a Function of Frequency

Since White Dwarf binaries have existed in stable orbits for millions of years, their gravitational wave emission is nearly monochromatic, meaning that their signal persists over extended timescales without significant frequency evolution. The gravitational wave frequency for a binary system is given by:

$$f = \frac{2}{P} = \frac{1}{\pi} \sqrt{\frac{GM}{a^3}} \quad (2.7)$$

where P is the orbital period of the binary, a is the semi-major axis, and M is the total mass of the binary system [23].

For compact binaries with orbital separations on the order of solar radii R_\odot , the resulting grav-

itational wave frequencies fall within the millihertz regime (mHz), aligning precisely with LISA's sensitivity range. The frequency evolution of a gravitational wave-emitting system is governed by[24]:

$$\frac{df_{GW}}{dt} = \frac{96}{5} \pi^{8/3} \left(\frac{G\mathcal{M}}{c^3} \right)^{5/3} f_{GW}^{11/3} \quad (2.8)$$

This equation demonstrates that higher-frequency binaries experience faster frequency evolution, whereas low-frequency binaries contribute to a persistent confusion noise background. The outputs were used to generate a population-wide spectrum of WDBs, allowing us to estimate the cumulative gravitational wave signal at different frequency bands.

Subtracting Strong Signals

A major challenge in constructing the White Dwarf gravitational wave background is the presence of strong individual sources that can obscure weaker signals. These strong signals must be subtracted or accounted for to ensure that the background model accurately represents the cumulative contribution from unresolved sources.

To perform signal subtraction, the strongest resolvable binaries were first identified based on their signal-to-noise ratio (SNR), given by:

$$SNR = \frac{h}{h_n} \quad (2.9)$$

where h_n is the noise spectral density at the given frequency. Binaries exceeding a predetermined SNR threshold were removed from the confusion background to prevent contamination. SNR quantifies the detectability of a gravitational wave source against instrumental and astrophysical noise. SNR for a given binary system is defined as [25]:

$$SNR^2 = 4 \int_{f_{min}}^{f_{max}} \frac{|\tilde{h}(f)|^2}{S_n(f)} df \quad (2.10)$$

where \tilde{h} is the Fourier transform of the gravitational wave strain, $S_n(f)$ is the power spectral

density (PSD) of the detector noise at frequency f and, f_{min}, f_{max} are the integration limits, corresponding to the sensitivity range of the detector.

This equation shows that the SNR depends on both the gravitational wave strain amplitude and the instrumental noise characteristics across the frequency band where the source emits.

For a binary system emitting nearly monochromatic gravitational waves, the SNR can be approximated using the characteristic strain:

$$SNR = \frac{h_c(f)}{\sqrt{S_n(f)}} \quad (2.11)$$

where $h_c(f)$ is the characteristic strain, and it can be given as:

$$h_c(f) = h\sqrt{fT_{obs}} \quad (2.12)$$

h is the intrinsic gravitational wave strain, and T_{obs} is the observational time, which enhances detectability over long-duration signals.

Since LISA observes low-frequency, long-lived gravitational wave sources, the observation time T_{obs} significantly enhances the SNR, making it possible to detect even relatively weak signals given sufficient integration time.

2.2.3 LEGWORK: Gravitational Wave Signal Modeling

Overview

LEGWORK is a Python-based package designed to compute gravitational-wave observables for compact binary systems, with a particular focus on space-based detectors such as LISA[26]. While COSMIC provides the astrophysical foundation by evolving binary populations through their stellar lifetimes, LEGWORK enables the translation of these evolved parameters into quantities relevant to gravitational wave detection. These include strain amplitudes, characteristic strain spectra, orbital frequency evolution, and signal-to-noise ratios (SNR). LEGWORK was critical in bridging

the gap between theoretical population synthesis and LISA’s instrumental observables, enabling detailed signal modeling for each binary in the synthetic population.

Integration with COGSWORTH Output

The interface between COGSWORTH and LEGWORK relies on a set of core binary properties: component masses, orbital periods (or equivalently, orbital separation), and distance. These quantities were extracted from the COGSWORTH output and passed as inputs to LEGWORK’s modeling functions. The outputs from COGSWORTH—including component masses, orbital periods, and distances—served as the foundational input for LEGWORK. Each system was assumed to follow a circular orbit, an approximation justified by the strong circularization effect of gravitational wave radiation in tight compact binaries. These properties were passed into LEGWORK’s *Source* class, which internally manages physical constants, unit conversions, and access to strain and SNR computation routines. The choice to assume circular, stationary systems simplifies the modeling process while remaining physically realistic for the majority of double white dwarf systems expected to be present in the LISA band. The *Source* object provides a streamlined interface for passing COSMIC data directly into LEGWORK’s analysis pipeline, allowing each binary to be analyzed individually while maintaining consistency across the simulated population.

Characteristic Strain

The characteristic strain h_c , as explained in Eq.(2.12), which quantifies the effective strength of a gravitational wave signal as observed over a finite time, was computed for each binary using LEGWORK’s *get_h_c_n* method. This calculation accounts for both the binary’s intrinsic gravitational wave strain and the duration of observation—in this case, a four-year LISA mission.

The strain values were computed based on the gravitational wave frequency (converted from orbital period), the chirp mass of the binary, and the assumed source distance (typically fixed at 10 kpc). These characteristic strain values serve as a direct input to the strain-frequency distribution, allowing the construction of a composite gravitational wave spectrum for the simulated galactic

population. This spectrum forms the empirical basis for the background fitting models developed in Section 2.2.5.

By applying this computation across tens of thousands of systems, LEGWORK enables statistical population-level analysis of the confusion foreground, while preserving the ability to isolate and assess individual systems where needed.

Signal-to-Noise Ratio

To determine whether a gravitational wave signal from a given binary would be detectable by LISA, LEGWORK’s *get_snr* function was used. This function calculates the signal-to-noise ratio (SNR) for a circular, non-evolving binary, integrating the signal power over LISA’s noise power spectral density. The LISA sensitivity curve was generated using the *lisa_psd* function from the *legwork.psd* module, ensuring consistency with mission design specifications.

The SNR values obtained for each binary were used to classify the population. Systems with $SNR \geq 7$ were considered resolvable and were excluded from the confusion foreground model, as their contribution would be removed in a realistic data analysis pipeline. Systems below this threshold were retained and treated as contributors to the unresolved foreground, whose aggregate signal was modeled and analyzed in subsequent sections.

This step was critical not only for foreground-background separation but also for constraining the amplitude and slope of the fitting models that describe the stochastic gravitational wave signal observable by LISA.

Integration in Workflow

LEGWORK played a pivotal role in transforming raw astrophysical data into gravitational wave observables. Its use enabled the construction of a population-wide strain spectrum, and its SNR calculations allowed the identification and removal of resolvable sources from the dataset.

The outputs from LEGWORK—frequency, characteristic strain, and SNR—were binned in logarithmic frequency space and used to construct a smooth spectral profile of the unresolved

foreground. This spectrum was then fitted using analytical models (see Section 2.2.5), allowing for direct comparison between simulation outputs and theoretical expectations for LISA.

By acting as the gravitational wave modeling engine in the overall pipeline, LEGWORK ensured that the signal properties of each COGSWORTH-evolved binary could be rigorously assessed and meaningfully interpreted within the context of detector sensitivity, mission duration, and source classification.

2.2.4 Cogsworth

Overview

Cogsworth is a Python-based framework designed to embed stellar populations within galactic structures, enabling astrophysical simulations to account for the spatial distribution and formation history of compact binaries. While COSMIC provides physically motivated binary evolution outputs, and LEGWORK computes their gravitational wave signatures, Cogsworth adds an essential astrophysical dimension: the placement of these systems within a realistic galactic context.

In this study, Cogsworth was used to post-process selected populations of White Dwarf binaries produced by COSMIC. The goal was to assign spatial coordinates, formation times, and star formation histories (SFH) to each system, allowing for more realistic modeling of source distances and merger rates across the Milky Way. This embedding step is critical for stimulating the white dwarf foreground observable by LISA, which is shaped not only by intrinsic binary properties but also by their distribution throughout the galactic disk and bulge.

Population Embedding and Star Formation History

Cogsworth supports a range of star formation models and galactic potentials. In this project, the Wagg2022 star formation history (SFH) [27] was used, coupled with the MilkyWayPotential [28] gravitational model. This configuration allows for a disk-dominated white dwarf binary population, consistent with current observations and theoretical expectations. The SFH defines when binaries form over cosmic time, while the galactic potential assigns spatial coordinates consistent

with the expected distribution of stars in the Milky Way.

Each system was assigned a birth time and position based on the chosen SFH and galactic structure. The spatial embedding enabled the calculation of line-of-sight distances from Earth for each system, which were later used in the LEGWORK strain and SNR computations. This step marked a transition from an abstract, volume-limited synthetic population to one that is spatially and temporally consistent with known stellar populations.

Output Integration and Use in Simulation

The output of COGSWORTH is a population object containing all original binary properties from COSMIC, augmented with 3D spatial coordinates, birth times, and assigned galactic distances. These embedded populations were exported as DataFrames and subsequently used to:

1. Assign realistic distances to binaries for strain calculations in LEGWORK,
2. Model spatial clustering effects in the galactic disk,
3. Filter populations by spatial criteria, such as those within 20 kpc from the Galactic Center.

Although not all COSMIC populations used in this study were embedded, key representative subsets were passed through COGSWORTH to verify distance distributions and support population-level modeling. This ensured that the simulated white dwarf background accounts for geometric and astrophysical effects that shape the gravitational wave foreground as seen by LISA.

2.2.5 Fitting Models

The construction of an accurate fitting model is essential for parameterizing the gravitational wave background generated by White Dwarf binaries (WDBs). Given the complexity of the simulated population and the wide frequency range over which these binaries emit, a mathematical model is required to describe the expected gravitational wave strength as a function of frequency. Fitting models allow for the extraction of key trends from COGSWORTH simulations, facilitating comparisons between theoretical and observational expectations for LISA. While previous studies have

employed power-law and exponential decay models, a refined approach is needed to capture better the astrophysical characteristics of WDBs and their collective influence on the gravitational wave background. This section details the rationale behind understanding fitting models, explores possible parameters, and discusses the challenges associated with accurately modeling the underlying astrophysical processes.

Importance of Fitting Models

Fitting models is an essential aspect of this study. Gravitational wave signals from White Dwarf binaries form a complex background that needs to be parameterized mathematically for analysis. The appropriate fitting models allow us to extract meaningful trends by approximating how GW signals behave across frequencies. They reduce the computational complexity in large-scale analyses by helping to separate astrophysical signals from noise. They improve our understanding by creating a parameterized function describing gravitational wave strength as a function of frequency and assist in identifying key trends, deviations, and unresolved features. They enable comparison between simulated results and theoretical expectations. Previous models have used exponential, power-law, and polynomial fittings, and we will attempt to refine or introduce a new approach.

Review of Existing Model

Accurately characterizing the unresolved gravitational wave background from compact binaries is crucial for understanding the low-frequency landscape LISA will observe. Several fitting models have been proposed in the literature to describe this background, typically relying on power-law behavior at low frequencies with a turnover at higher frequencies where instrumental sensitivity dominates or where source populations thin out. One of the most widely adopted models in this context is the formulation presented by Cornish and Robson (2019)[29]. Their model captures the essential features of the galactic white dwarf foreground by combining a simple power-law behavior with a smooth high-frequency turnover. The Cornish and Robson model has been shown to fit synthetic white dwarf backgrounds well across various galactic realizations and serves as a

standard reference for LISA foreground studies. Given its proven success and its physical interpretability, the Cornish and Robson model was selected as the baseline fitting framework for this study. Subsequent sections describe its mathematical form, adaptations made to tailor it to the simulation outputs generated here, and challenges encountered during the fitting process.

Mathematical Formulation of the Galactic Confusion Noise Model(Cornish et al. 2019)

The Galactic Confusion Noise describes the cumulative gravitational wave signals from unresolved white dwarf binaries within the Milky Way. Following the model proposed by Cornish et al. (2019), the confusion noise spectral density $S_c(f)$ is mathematically represented by:

$$S_c(f) = Af^{-7/3}e^{-f\alpha+\beta f \sin(\kappa f)}[1 + \tanh(\gamma(f_k - f))] \text{ Hz}^{-1} \quad (2.13)$$

This functional form encapsulates the complex behavior of confusion noise, characterized by a steep spectral dependence, frequency modulation, and an exponential tapering at higher frequencies.

Parameters of the Model:

For a standard LISA mission duration of four years, the fitting parameters are set as follows:

| Parameter | Description | Value (4 year mission) |
|-----------|-----------------------------------|------------------------|
| A | Overall amplitude scaling factor | 9×10^{-45} |
| α | High-frequency exponential cutoff | 0.138 |
| β | Frequency modulation strength | -221 |
| κ | Frequency modulation periodicity | 521 |
| γ | Cutoff steepness factor | 1680 |
| f_k | Characteristic knee frequency | 0.00113 Hz |

Table 2.1: Parameters of Cornish et al. 2019

The Physical interpretation:

- The $f^{-7/3}$ dependence originates from gravitational wave emission theory, reflecting the dominant quadrupole emission expected from compact binaries.
- The exponential term $e^{-f\alpha}$ imposes a smooth high-frequency cutoff.

- The sinusoidal modulation $\sin(\kappa f)$ captures subtle frequency-dependent oscillations due to the varying spatial distribution of binary sources in the galaxy.
- The hyperbolic tangent term $[1 + \tanh(\gamma(f_k - f))]$ smoothly transitions the noise spectrum around a knee frequency f_k , below which confusion noise dominates.

This model is particularly critical in gravitational-wave data analysis for space-based detectors like LISA, where confusion noise significantly affects the detectability of weaker signals.

2.2.6 Schematic overview of the gravitational wave foreground modeling pipeline.

To provide a comprehensive view of the entire foreground modeling process, Figure 2.1 presents a schematic representation of the pipeline developed in this study. The framework begins with COSMIC, which performs population synthesis to generate compact binary systems. These are then passed to COGSWORTH, which embeds them into a realistic galactic environment using the Wagg2022 star formation history and the Milky Way potential, producing synthetic galaxy populations that are astrophysically grounded.

The pipeline proceeds by extracting these evolved populations using custom scripts (*generation.py*) and batching them into large-scale .parquet files. These batches are merged and processed to isolate unresolved binaries—those that fall below LISA’s detection threshold. Using LEGWORK, each system’s characteristic strain and gravitational wave frequency are calculated. The unresolved population is then binned in strain-frequency space to form the raw data used for foreground modeling.

The final stage involves fitting analytic models to the power spectral density of the unresolved foreground. Two fitting procedures are applied: one using parameter bounds centered on the canonical Milky Way values, and another without any constraints, allowing the model to freely capture the shape of each galaxy’s unresolved foreground. This modular and reproducible pipeline supports both astrophysical realism and interpretive flexibility, and forms the backbone for all subsequent analyses presented in Chapters 3 and 4.

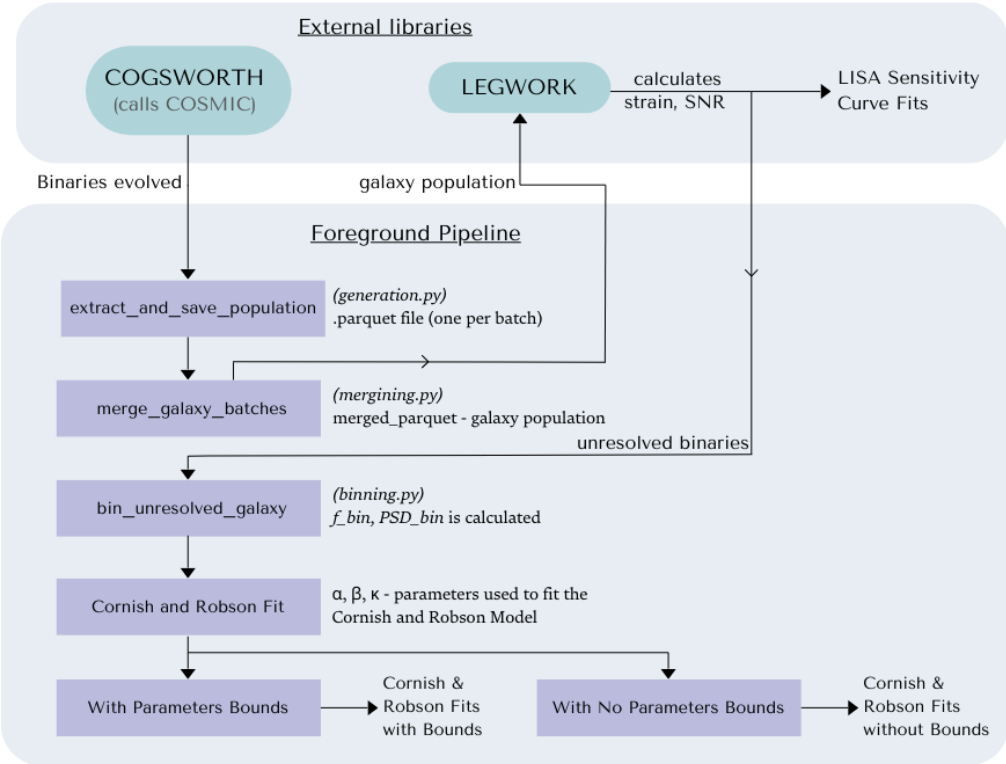


Figure 2.1: Schematic overview of the gravitational wave foreground modeling pipeline. External libraries such as COSMIC, Cogsworth, and LEGWORK were integrated to simulate binary evolution, embed galaxy populations, and compute unresolved background signals.

2.2.7 Data & Code Availability.

All simulation scripts, analysis notebooks, and plotting utilities referenced in this thesis are archived at `GW_foreground_LISA`.

2.3 Simulations

This section documents the computational infrastructure and workflow used to execute population synthesis and gravitational wave modeling tasks at scale. Due to the size and complexity of the simulated white dwarf binary populations, especially those requiring Monte Carlo realizations and LEGWORK-based post-processing, high-performance computing (HPC) resources were utilized.

All large-scale simulations were run on the Quest computing cluster at Northwestern University.

2.3.1 Quest: High-Performance Computing (HPC) Setup

Overview of Quest

Quest is Northwestern University’s shared HPC cluster, designed to support data-intensive and compute-heavy scientific workflows. It offers a range of computing nodes equipped with multicore CPUs, high-memory configurations, and support for parallel job submission using the SLURM workload manager. Quest was selected for its scalable resources, interactive environment, and support for long-running Python jobs, which aligned with the needs of COGSWORTH and LEGWORK simulations.

Simulation Workflow on Quest

Due to the computational requirements of generating a large galaxy-embedded binary population ($\sim 10^7$ binaries per galaxy), a batch-based simulation workflow was implemented on the Quest HPC cluster. This workflow utilized SLURM job scripts to automate population sampling and batch file management. Each galaxy population simulation was divided into multiple batches, with each batch containing 20,000 binaries, resulting in 200 arrays of files. This approach allowed for parallelization and better resource utilization without overwhelming the available memory on a single Quest node. This allowed multiple such simulations to run at the same time, thus making it easier to have a very efficient system for the sequential production of galaxy populations.

Resource Allocation

Typical runs were configured with:

1. 8 CPUs per job with 16–32 CPU cores
2. 20 GB of RAM per job
3. Walltime: 20 hours for the whole job (1 hour for one array)

4. No GPU was required, as Cogsworth and LEGWORK are CPU-bound

5. Modules: Anaconda environment with Cogsworth installed

SLURM Job Script

A standard SLURM job script was created for each galaxy, such as *g1010_014.slurm*. The job script specified computational resources and executed a batch generation Python script. A typical configuration included:

```
#!/bin/bash

#SBATCH --account=b1094 # Your allocation/account name
#SBATCH --partition=ciera-std # Partition name
#SBATCH --job-name=binary_batch_test # Job name
#SBATCH --array=0-199           # Run 200 jobs: batch 0 to 199
#SBATCH --ntasks=1              # Only 1 task per job
#SBATCH --cpus-per-task=8       # Use 8 CPUs per job
#SBATCH --mem=20G               # Memory per job
#SBATCH --time=01:00:00          # Max time per job
#SBATCH --output=logs/g1010_014_%A_%a.out      # Standard output
#SBATCH --error=logs/g1010_014_%A_%a.err        # Error log output
#SBATCH --mail-user=neelpanchal2025@u.northwestern.edu # Email
#SBATCH --mail-type=BEGIN,END,FAIL # receive job notifications

# --- Run Python script with batch index ---
# Force Python to use conda binary explicitly
/home/kxy1597/.conda/envs/cogsworth/bin/python generate_batch.py
--batch-index ${SLURM_ARRAY_TASK_ID}
```

The `--array=0-199` flag enabled submission of 200 independent batch jobs, each generating a subset of the final galaxy population. This structure ensured full coverage while reducing individual job memory and runtime demands. Each SLURM task invoked `generate_batch.py`, a Python script that loaded the fixed COSMIC population, sampled binaries using COGSWORTH’s `create_population()`, and saved the result as an individual `.parquet` file.

Python Scripts for Batch Processing

The `generate_batch.py` script was responsible for:

- Loading the fixed COSMIC input population (Evolved in COGSWORTH)
- Sampling n_{batch} binaries according to galactic star formulation history and potential
- Call out the `extract_and_save_population()` from `extract_utils.py` file.

Once all batch jobs completed, the `extract_utils.py` script was used to:

- Load the generated batch files from a batch directory
- Select `.bpp` and `.final_pos` from `population` Object and slice them for individual arrays
- Concatenate them into a single, unified `.parquet` file for the particle population
- Saving each batch as a `.parquet` file with filenames reflecting the batch index
(e.g.`g1010_014_0000_bpp_with_pos.parquet`.)

2.3.2 Simulation Overview and Model Variants

To model the gravitational wave background arising from compact white dwarf binaries, eight distinct simulation sets were generated by sampling pre-evolved COSMIC populations using COGSWORTH. Rather than directly evolving binaries from primordial parameters, this study utilized COSMIC’s fixed, evolved populations, which represent detached double white dwarf systems at late evolutionary stages. COGSWORTH’s sampling functions were then employed to select binaries from

these populations and embed them within a realistic galactic model. Each simulation was configured with a unique combination of white dwarf types and progenitor metallicities, allowing for a comprehensive exploration of parameter space most relevant to LISA’s millihertz sensitivity band. The simulations were designed to account for how stellar composition and metallicity affect binary evolution outcomes, gravitational wave emission strength, and ultimately, population-level observability.

The four combinations explored included:

1. Double helium white dwarfs (He+He ; $\text{kstar_1} = 10$, $\text{kstar_2} = 10$)
2. Carbon-oxygen + helium white dwarfs (CO+He ; $\text{kstar_1} = 11$, $\text{kstar_2} = 10$)
3. Double carbon-oxygen white dwarfs (CO+CO ; $\text{kstar_1} = 11$, $\text{kstar_2} = 11$)
4. Oxygen-neon + helium or CO white dwarfs (ONe+He/CO ; $\text{kstar_1} = 12$, $\text{kstar_2} = 10$ and 11)

The eight simulation sets explored combinations of white dwarf core compositions, defined by the kstar classifications, across two progenitor metallicities. Specifically, the binary configurations included He+He, CO+He, CO+CO, and ONe+He systems, each modeled at both solar metallicity ($Z = 0.0021$) and a lower metallicity ($Z = 0.014$). These combinations allow for the investigation of how stellar composition and metallicity influence binary formation outcomes, chirp mass distributions, and gravitational wave strain amplitudes in the LISA band.

Following the sampling of binary populations, Cogsworth assigned each system a formation time and a three-dimensional galactic position according to the Wagg2022 star formation history and MilkyWayPotential gravitational potential. This step transformed the synthetic populations into a spatially distributed galaxy model, enabling realistic modeling of distance-dependent gravitational wave observables.

Each galaxy-modeled population was saved as a `.parquet` file, with filenames reflecting the kstar combination and metallicity (e.g., `g1010_z_0.014.parquet`). These embedded populations

formed the basis for all subsequent gravitational wave signal modeling and background fitting described in later sections.

| Galaxy Name | kstar_1 | kstar_2 | White Dwarf Type | White Dwarf Type | Metallicity (z) |
|-------------|---------|---------|------------------|------------------|---------------------|
| g1010_014 | 10 | 10 | He | He | 0.014 |
| g1110_014 | 11 | 10 | CO | He | 0.014 |
| g1111_014 | 11 | 11 | CO | CO | 0.014 |
| g1210_014 | 12 | 10,12 | ONe | He+ONe | 0.014 |
| g1010_0021 | 10 | 10 | He | He | 0.0021 |
| g1110_0021 | 11 | 10 | CO | He | 0.0021 |
| g1111_0021 | 11 | 11 | CO | CO | 0.0021 |
| g1210_0021 | 12 | 10,12 | ONe | He+ONe | 0.0021 |

Table 2.2: Summary of COGSWORTH simulations used in this study, categorized by kstar type, white dwarf composition, and progenitor metallicity.

The inclusion of low-metallicity variants is motivated by the influence of metallicity on stellar winds and mass loss during evolution, which in turn alters the binary’s final orbital parameters and gravitational wave emission. Lower-metallicity populations may favor more compact post-common-envelope systems, which will result in stronger gravitational wave signals for a given chirp mass. The (12 & 10, 12) configuration, representing $ONe + He$ binaries, was also included despite its rarity, as such systems may contribute significantly at higher frequencies and offer insights into more massive, short-period white dwarf binaries.

Together, these eight simulations serve as the foundation for modeling the unresolved galactic foreground in the LISA band. They provide coverage across core compositions and initial conditions, forming a diverse but astrophysically grounded parameter space. The resulting datasets provide the foundation for all subsequent modeling of the unresolved foreground, signal subtraction, and fitting model development presented in Chapters 2 and 3.

2.3.3 Simulation Post-processing and Gravitational Wave Calculations

Loading Embedded Population Data

The post-processing analysis begins by loading galaxy-embedded white dwarf binary populations generated using COSMIC and COGSWORTH. Each simulated population is stored in a structured *.parquet* file, ensuring efficient handling of large datasets typically comprising millions of binary systems. The *.parquet* file format was selected due to its optimized compression and fast data retrieval, critical for handling large-scale simulations. These files primarily consist of two key data structures:

- Binary Population Parameters(bpp): Containing detailed evolutionary parameters of each binary system, including stellar masses (m_1, m_2), evolutionary states (kstar types), and orbital parameters (eccentricity (ecc), orbital period ($porb$))).
- Final Position/Velocities (final_pos): Final states of binaries stored in an array format of 3 dimensions. It is instrumental for cases where complete orbits are not required.

Due to computational resource constraints and the large-scale nature of the simulations (generating approximately 10^7 binaries per galaxy), populations were simulated in smaller batches of 50,000 binaries each, leveraging SLURM-managed parallel computations on the Quest HPC cluster. After completing these batch runs, individual output *.parquet* files were systematically concatenated into comprehensive galaxy-wide datasets. This concatenation process was performed using Python scripts employing Pandas for efficient merging, resulting in unified, consistent population files (e.g., combining individual batch outputs into a single *g1010_0.014.parquet* file). This approach optimized computational efficiency while maintaining data integrity and consistency throughout the post-processing pipeline.

Population Filtering and Parameter Extraction

After loading the complete galaxy-wide datasets, rigorous filtering criteria were applied to extract physically relevant binary populations suitable for gravitational wave analysis. Initially, the

data were systematically sliced to retain only key parameters crucial for subsequent calculations, including stellar masses (m_1, m_2), orbital periods, eccentricities, and galactic spatial coordinates (x, y, z).

To ensure physical realism, binary populations were filtered based on the following criteria:

- **Binary Type Consistency:** Binaries were restricted to specific stellar evolution endpoints (e.g., double white dwarfs, represented by kstar types 10, 11, 12).
- **Removal of Non-physical Values:** Systems exhibiting negative mass values, extreme orbital eccentricities, or unrealistic orbital periods were systematically excluded.
- **Frequency Range Relevance:** Binaries with gravitational wave frequencies outside LISA's sensitive detection band (approximately 10^{-4} Hz to 1 Hz) were removed to streamline downstream computations.

These filtering operations were efficiently implemented in Python using Pandas, exploiting vectorized operations for rapid data handling. The refined datasets significantly reduced computational complexity, focusing subsequent gravitational wave observable calculations strictly on viable binary candidates.

The final pipeline was critical for enhancing computational efficiency and ensuring that subsequent gravitational wave calculations and parameter estimations were accurate and physically meaningful.

Calculation of Gravitational Wave Observable

With the filtered and physically consistent binary populations prepared, gravitational wave observables were systematically calculated. These observables included the gravitational wave frequency (f_{GW}), characteristic strain (h_c), and the corresponding signal-to-noise ratio (SNR), each essential for evaluating binary detectability within the LISA sensitivity range.

The gravitational wave frequency for circular binaries was computed directly from orbital pe-

riod data (P_{orb}) using the relation:

$$f_{GW} = \frac{2}{P_{orb}} \quad (2.14)$$

Characteristic strain (h_c) was then calculated following:

$$h_{c,n}^2 = \left(\frac{f_n^2}{\dot{f}_n} \right) h_n^2. \quad (2.15)$$

To account for the integration of the signal over the LISA mission, we instead use the ‘characteristic’ strain amplitude of the n^{th} harmonic, $h_{0,n}$, which is the term present in the general signal-to-noise ratio equation. This can be related to the strain amplitude in the n^{th} harmonic, $h_{0,n}$, as mentioned in [30] [31]. The characteristic strain represents the strain measured by the detector throughout the mission (approximated as a single broadband burst), whilst the strain amplitude is the strength of the GW emission at each instantaneous moment.

The SNR was computed by integrating the ratio of the squared characteristic strain to the LISA sensitivity spectral density $S_n(f)$, as:

$$SNR^2 = \int \frac{h_c^2(f)}{f S_n(f)} d(\ln f) \quad (2.16)$$

with the integral performed numerically over the relevant LISA frequency range. The Cornish et al. (2019) model, incorporating both instrumental and galactic confusion noise, defined the baseline sensitivity $S_n(f)$ used in these calculations.

These computations were executed efficiently in Python, utilizing NumPy and SciPy libraries for numerical integration and vectorized calculations for rapid processing. The resulting observable datasets formed the foundation for subsequent analyses, including source detectability assessments and confusion noise fitting.

2.3.4 Data Management and Workflow Automation

Given the enormous volume of binaries generated across multiple galaxy simulations, structured data management and automated workflows were critical to maintaining consistency, traceability, and computational efficiency throughout the analysis pipeline. The initial populations, generated in discrete batches to overcome HPC resource limitations, were concatenated post-simulation into a single unified *.parquet* file per galaxy, as described in Section 2.3.3.1.

Automated Python scripts were developed to standardize the following tasks:

- Batch File Concatenation: Sequentially merging multiple small batch outputs into a complete galaxy population using Pandas, ensuring no loss of data fidelity.
- Filtering and Preprocessing Pipelines: Automating the application of physical filters (binary type, orbital parameters) immediately after loading each concatenated file.
- Observable Calculations: Streamlining the calculation of f_{GW}, h_c , and SNRs for millions of binaries using efficient vectorized operations.
- Storage and Organization: Processed datasets, gravitational wave observables, and intermediate results were consistently saved with descriptive filenames, allowing for reproducibility and easy retrieval during later stages of fitting and visualization.

The entire workflow was designed to minimize manual intervention, ensuring reproducibility across simulations and facilitating rapid updates or re-runs when parameter adjustments were needed. Moreover, careful version control of scripts and results ensured that analyses could be reliably traced back to specific simulation configurations, enhancing the scientific rigor of the study.

CHAPTER 3

RESULTS

In this chapter, the results of the simulated galactic populations are presented, focusing on the detectability of compact binary systems and the modeling of the unresolved gravitational wave foreground. Trends across different stellar types and metallicities are explored, providing a detailed view of both individual sources and the broader confusion noise landscape relevant for future LISA observations.

3.1 Overview of Simulated Galactic Population

The gravitational wave foreground was constructed using eight distinct galaxy populations, each representing different combinations of white dwarf evolutionary channels and metallicity values. These populations were generated by evolving 10^7 binary systems per galaxy using COSMIC and embedding the resulting systems into a synthetic Milky Way potential with Cogsworth.

After population synthesis and galactic embedding, gravitational wave observables—including gravitational wave frequency (f_{GW}), characteristic strain (h_c), and signal-to-noise ratio (SNR)—were calculated for each system. Detectable sources were defined as those achieving an SNR more significant than 7 over the nominal 4-year LISA mission lifetime.

The resulting datasets, described in Table 3.1, provide the foundation for characterizing individually detectable sources and analyzing the unresolved stochastic foreground, forming the basis for confusion noise modeling presented in subsequent sections.

3.2 Detectable Sources in Simulated Galactic Population

Following the computation of gravitational wave observables for the embedded white dwarf binary populations, sources were classified based on their detectability with the Laser Interferometer

| Galaxy | kstars | Type | metallicity (z) | $m_1 (M_\odot)$ | $m_2 (M_\odot)$ | No. of Binaries |
|------------|------------|--------------|-----------------|-----------------|-----------------|-----------------|
| g1010_014 | 10 - 10 | He - He | 0.014 | 21.11 | 25.28 | 9927626 |
| g1110_014 | 11 - 10 | He - CO | 0.014 | 20.40 | 26.93 | 9970268 |
| g1111_014 | 11 - 11 | CO - CO | 0.014 | 19.71 | 26.3 | 9759505 |
| g1210_014 | 12 - 10,12 | ONe - He, CO | 0.014 | 21.93 | 23.68 | 9718273 |
| g1010_0021 | 10 - 10 | He - He | 0.0021 | 24.82 | 25.26 | 10080084 |
| g1110_0021 | 11 - 10 | He - CO | 0.0021 | 24.10 | 23.41 | 9812049 |
| g1111_0021 | 11 - 11 | CO - CO | 0.0021 | 22.60 | 23.43 | 9657244 |
| g1210_0021 | 12 - 10,12 | ONe - He, CO | 0.0021 | 23.07 | 21.10 | 9717164 |

Table 3.1: Overview of 8 galaxy populations

Space Antenna (LISA). A detection threshold was applied, defining detectable sources as those with a signal-to-noise ratio (SNR) greater than seven over the assumed four-year observation period.

For each of the eight simulated galactic populations, the gravitational wave signals of individual binaries were compared against the LISA sensitivity curve, incorporating both instrumental noise and the modeled galactic confusion noise. Only systems exceeding the detection threshold across their gravitational wave frequency evolution were selected.

Detectable sources predominantly consist of high-mass binaries and systems with short orbital periods, both of which contribute stronger gravitational wave signals. The distribution of detectable systems varies with metallicity and the evolutionary endpoints (kstar types) of the binaries, reflecting differences in mass distributions, merger rates, and orbital separations across the populations.

Plots of the detectable sources for each galaxy are presented, overlaid on the LISA sensitivity curve. These visualizations provide insight into the frequency range and strain amplitude where detection is most probable, as well as the overall contribution of each galaxy to the individually resolvable source population.

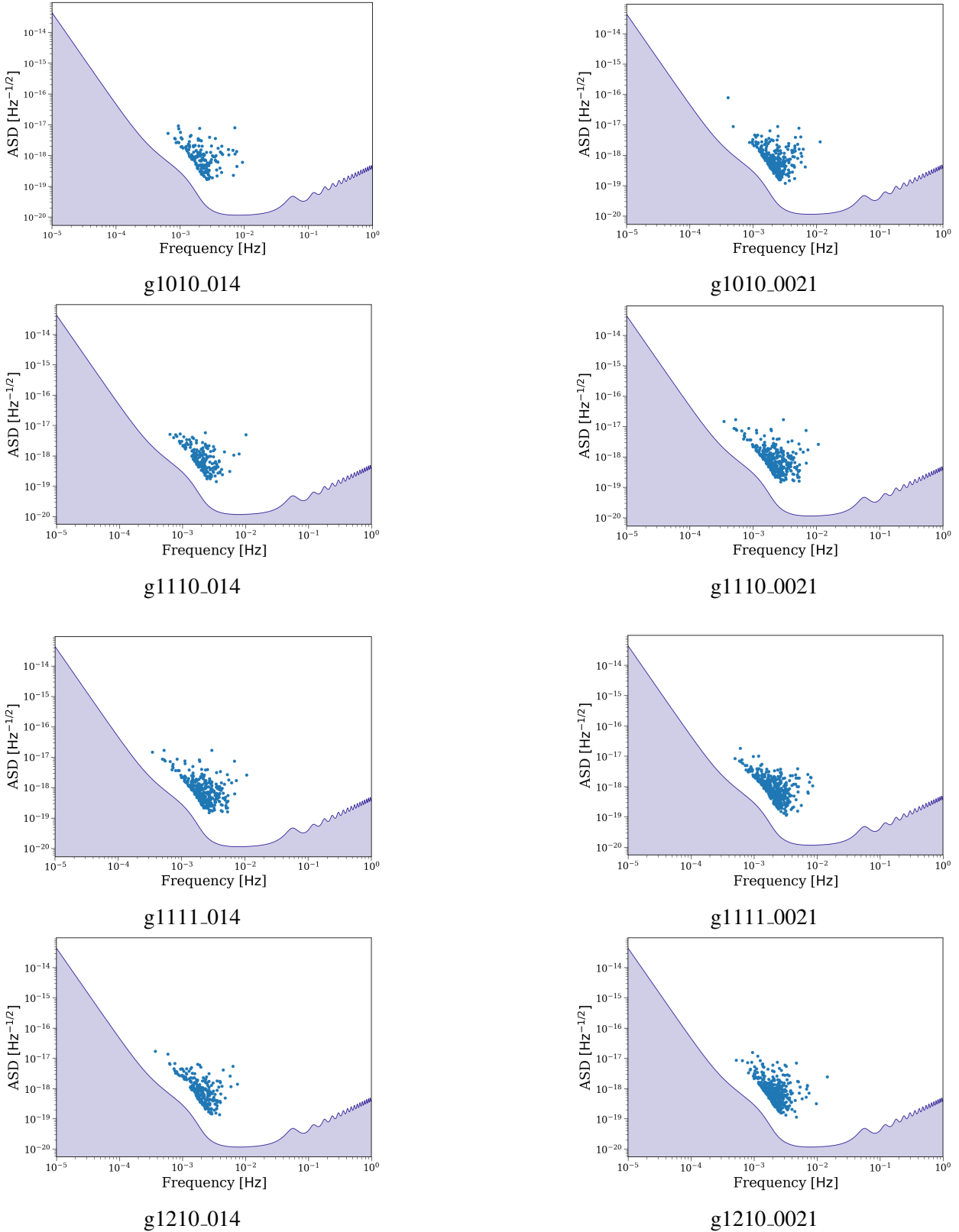


Figure 3.1: LISA sensitivity plots showing unresolved sources ($SNR > 7$) for each galaxy.

Each subplot overlays the individually detectable sources ($\text{SNR} > 7$) from a simulated galaxy onto the LISA sensitivity curve, shown as the shaded region. The x-axis represents the gravitational wave frequency, and the y-axis shows the amplitude spectral density (ASD), allowing direct visual comparison with the LISA detection threshold.

Across all eight simulations, the detectable systems predominantly cluster between 10^{-4} Hz and 10^{-2} Hz, corresponding to short-period white dwarf binaries with high orbital frequencies. The amplitude of these sources generally falls near or above LISA’s most sensitive band, highlighting that source detectability is concentrated in a narrow frequency window. Populations with higher primary kstar values (e.g., 11 or 12) and low metallicity tend to have slightly more scattered distributions, reflecting more diverse or extreme binary configurations.

Overall, while the number of detectable sources is small compared to the entire population (binaries), their concentration in a well-defined region of parameter space offers a strong foundation for confusion noise subtraction and model fitting in the subsequent sections.

3.3 Characteristic Strain vs. Gravitational Wave Frequency

The characteristic strain versus gravitational wave frequency plots for each galaxy reveal the population-level structure of unresolved white dwarf binaries across the LISA sensitivity band. These distributions offer more than visual summaries—they encode the astrophysical history and binary evolution outcomes of each synthetic population.

The densely populated triangular region spanning approximately $10^{-4} \leq f_{\text{GW}} \leq 10^{-2}$ Hz reflects the transition between weakly and strongly interacting compact binaries. At lower frequencies, systems evolve slowly due to weak gravitational radiation, leading to population buildup—this is often referred to as a “gravitational wave bottleneck”. In contrast, higher-frequency binaries, particularly those closer to Roche-lobe overflow or merger, are fewer but individually more substantial in h_c , and their signals begin to emerge above the LISA sensitivity floor.

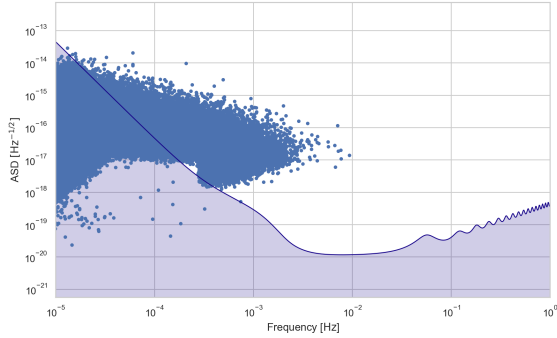
The upper envelope of the strain distribution corresponds to systems with higher chirp masses and tighter orbital separations. Notably, metallicity plays a significant role in shaping these edges:

low-metallicity environments promote the formation of more massive white dwarfs and tighter binaries due to reduced stellar winds and more efficient common envelope ejection. As a result, the $Z = 0.0021$ populations generally show both broader frequency coverage and a slight upward shift in strain at fixed frequency, compared to their solar-metallicity counterparts.

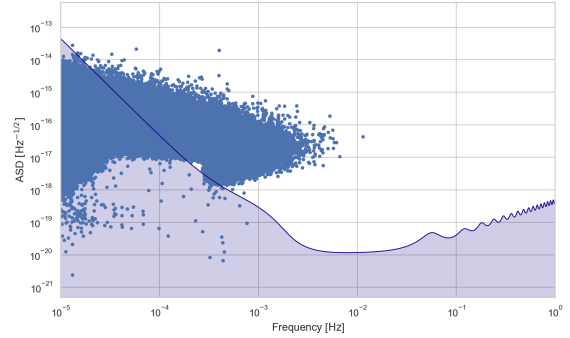
Another feature evident in these plots is the relative suppression of high-frequency sources in specific populations, especially those involving hybrid or ONe WDs (e.g., $kstar=12$). These systems often result in earlier mergers or enter mass-transfer phases before reaching high f_{GW} , explaining the tapering of strain density above 10^{-2} Hz.

Overall, these distributions lay the groundwork for confusion noise modeling. The unresolved binaries that fall below the detection threshold contribute to a persistent foreground, and the characteristic strain curves here provide the physical inputs required to fit analytic confusion noise models, such as those derived from Cornish et al. (2019), in subsequent sections.

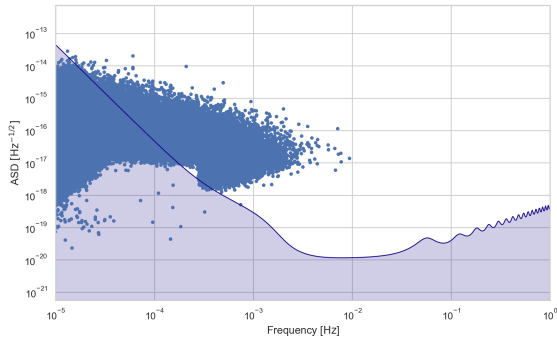
In addition to shaping the foreground, the distribution of sources in h_c - f_{GW} space also highlights the relative efficiency of LISA in different regimes. Systems clustered just below the sensitivity curve are prime candidates for marginal detection over longer mission durations or through improved data analysis techniques, such as matched filtering or stacking. Meanwhile, binaries lying well below the curve are unlikely to be individually resolved but contribute coherently to the gravitational wave background. The relative balance between these two populations will determine the statistical properties of the residual confusion noise, which motivates the detailed modeling efforts undertaken in the following sections. Table 3.2 depicts the same ideology across all eight galactic populations.



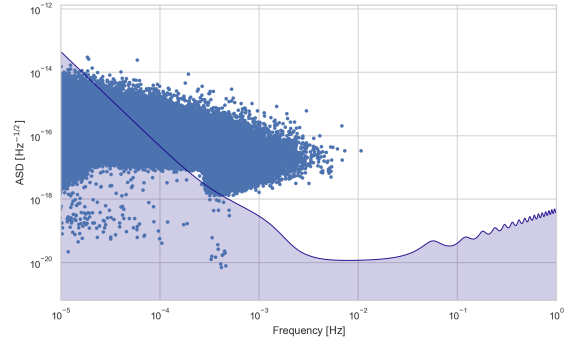
(a) g1010_014



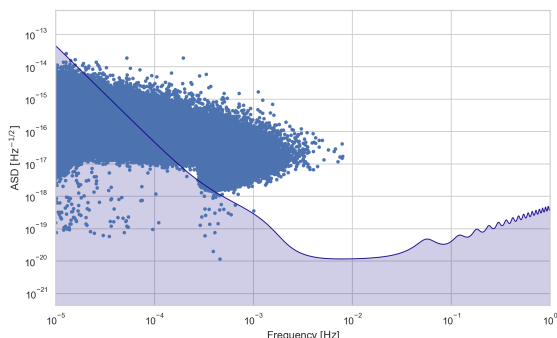
(b) g1010_0021



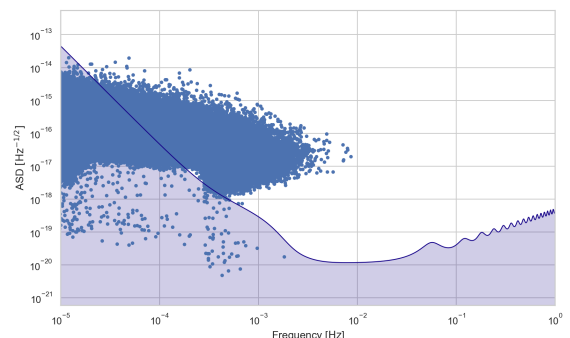
(c) g1110_014



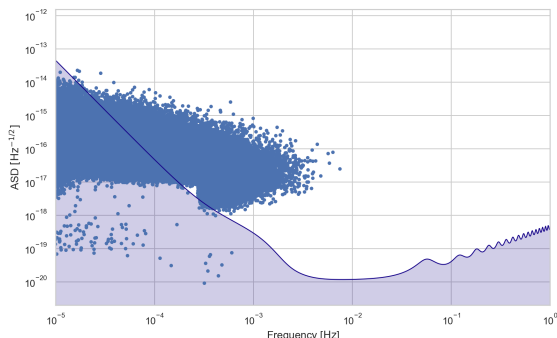
(d) g1110_0021



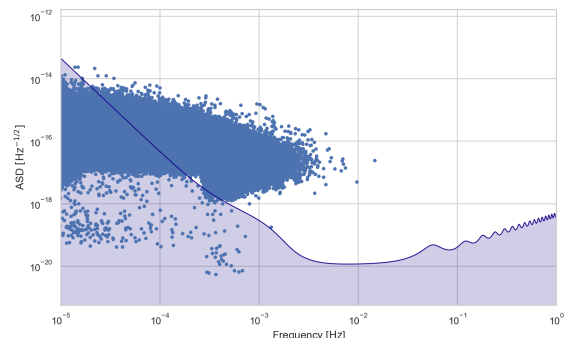
(e) g1111_014



(f) g1111_0021



(g) g1210_014



(h) g1210_0021

Figure 3.2: Strain vs. Gravitational Wave Frequency for each galaxy.

3.4 Fitting Galactic Confusion Noise

Following the calculation of gravitational wave observables for each galaxy population, the residual unresolved background, after removing strongly detectable sources with signal-to-noise ratio ($SNR > 7$), was modeled using a confusion noise fitting approach. The primary objective was to characterize the underlying stochastic gravitational wave background arising from the ensemble of unresolved binaries in each simulated galaxy.

The fitting procedure involved two complementary approaches:

- Baseline Comparison Using Pre-Computed Milky Way Model:

As a reference, the confusion noise model provided by the LEGWORK package was utilized. This model is based on a synthetic Milky Way population calibrated to observed galactic parameters and employs a version of the Cornish et al. (2019) fitting formula. The LEGWORK baseline served as a validation tool, ensuring that fitting results from the simulated galaxy populations were physically consistent with established models.

- Direct Fitting of Simulated Galaxy Populations:

Independently, the confusion noise for each simulated galaxy was fitted directly using the Cornish et al.(2019) model formulation:

$$S_c(f) = Af^{-7/3}e^{-f\alpha+\beta f \sin(\kappa f)}[1 + \tanh(\gamma(f_k - f))] \text{ Hz}^{-1} \quad (3.1)$$

where $A, \alpha, \beta, \kappa, \gamma$, and f_k are fitting parameters.

The fitting was performed using non-linear least squares methods (`scipy.optimize.curve_fit`), applied separately under two conditions:

- With parameters bounds: enforcing physically motivated limits on parameter ranges to stabilize the fitting process.

- Without parameter bounds: allowing maximum flexibility to explore how freely the simulated data deviates from idealized assumptions.

This dual approach (bounded vs. unbounded fitting) provided insight into the stability of the confusion noise characteristics across different galaxy models and metallicities. It highlighted the sensitivity of fitting parameters to underlying binary population properties. The fitted models, alongside the baseline LEGWORK confusion curve, are presented in the following sections, with detailed discussions of parameter variations and fitting quality.

3.5 Galactic Confusion Noise Model (Cornish et al. 2019) Fits

The post-subtraction confusion foreground, dominated by unresolved double white dwarf binaries, was quantitatively modeled using the parameterized functional form from Cornish et al. (2019). The model was applied to the binned characteristic strain distributions of each galaxy, treating the residual population as a stochastic source with a smooth spectral profile. The fitting was performed in logarithmic frequency space using a non-linear least squares optimizer. The model fitting was split into two regimes to assess robustness and degeneracy systematically:

- Section 3.5.1 imposes prior-informed parameter bounds to constrain the fits within astrophysically motivated ranges and suppress known degeneracies (e.g., between β and κ near the confusion turnover).
- Section 3.5.2 relaxes all parameter constraints to explore the sensitivity of the foreground shape to small-scale variations in the population distribution.

This dual-approach reveals not only how well the Cornish and Robson model captures the global foreground shape, but also the extent to which specific features (e.g., modulation depth, cutoff behavior) are artifacts of population synthesis assumptions or fitting flexibility.

3.5.1 Cornish and Robson Model Fits (With Parameter Bounds)

To quantitatively assess the spectral characteristics of the unresolved gravitational wave foreground produced by each synthetic population, we fit the analytical model proposed by Cornish et al. (2019) to the binned power spectral density (PSD) curves of the simulated unresolved sources. For this section, all fits were performed using parameter bounds centered on the values reported by Robson et al. (2019), which represent a calibrated model of the Milky Way foreground as derived from population synthesis using LEGWORK.

This modeling choice is not arbitrary. The galaxy populations used in this work were deliberately constructed to be Milky Way analogs. The COGSWORTH pipeline employed for galaxy modeling uses the Wagg et al. (2022) star formation history as its default — a parametrization explicitly designed to reflect the Milky Way’s evolutionary history across its thin disk, thick disk, and bulge components. In parallel, all populations were evolved within the Milky Way gravitational potential, as modeled in the galpy framework. The populations selected for fitting in this section represent specific evolutionary channels (as defined by kstar combinations) across two different metallicity environments, but all are derived from the same underlying physical assumptions and galactic context. As such, it is scientifically appropriate to compare their confusion foregrounds to the empirical Milky Way model and to constrain the parameter fitting within bounds reflective of that benchmark.

Each fitting routine was initialized with the Cornish and Robson et al. (2019) parameter values and allowed to vary within windows that reflect plausible physical deviations while remaining centered on Milky Way behavior. The motivation here was not only to test the performance of the Cornish et al. functional form on resolved simulations but also to examine the internal consistency of our galaxy generation and waveform modeling pipeline.

Strikingly, across all eight synthetic populations, five of the six parameters — specifically α (the exponential suppression exponent), β and κ (oscillatory phase modifiers), γ (tanh roll-off sharpness), and f_k (roll-off frequency) — closely converged to the Cornish and Robson et al. (2019) Milky Way values. The only parameter that consistently differed was the amplitude A ,

which emerged from the fits at approximately 5×10^{41} , in contrast to Cornish and Robson’s fixed value of 9×10^{45} . This deviation is expected: while Robson et al. fixed the amplitude based on normalization to a specific Milky Way simulation, our fitting procedure allowed A to vary freely within the bounds to better reflect the size and composition of the individual sub - populations analyzed here.

It is important to note that although each of these eight populations represents only a portion of a full galactic model — typically filtering systems by compact object type and metallicity — the consistency of the fitted spectral parameters suggests that each subset independently retains the overall spectral imprint of a Milky Way-like foreground. This indicates that the structural features of the confusion noise are not merely emergent properties of the full galaxy population, but rather intrinsic to the formation and evolution channels represented in our simulation.

Together, these results provide strong support for the physical realism of our pipeline. From COSMIC’s binary evolution modeling to COGSWORTH’s galactic embedding and LEGWORK’s waveform generation, the pipeline accurately reproduces known foreground structure at the level of individual sub-populations. Table 3.2 summarizes the best-fit parameters for each galaxy, and Figure 3.3 provides visual confirmation of the excellent agreement between the fitted models, the LEGWORK-derived PSDs, and the reference Cornish and Robson et al. (2019) curve.

| Galaxy | kstars | WD Type | Metallicity (z) | A |
|---------------|---------------|----------------|-------------------------------------|---------------------------|
| g1010_014 | 10 - 10 | He - He | 0.014 | 5.00005×10^{-41} |
| g1110_014 | 11 - 10 | He - CO | 0.014 | 5.00005×10^{-41} |
| g1111_014 | 11 - 11 | CO - CO | 0.014 | 5.00005×10^{-41} |
| g1210_014 | 12 - 10,12 | ONe - He, CO | 0.014 | 5.00005×10^{-41} |
| g1010_0021 | 10 - 10 | He - He | 0.0021 | 5.00005×10^{-41} |
| g1110_0021 | 11 - 10 | He - CO | 0.0021 | 5.00005×10^{-41} |
| g1111_0021 | 11 - 11 | CO - CO | 0.0021 | 5.00005×10^{-41} |
| g1210_0021 | 12 - 10,12 | ONe - He, CO | 0.0021 | 5.00005×10^{-41} |

Table 3.2: Cornish and Robson Parameters with Bounds on all eight galaxy populations.

These findings provide a compelling insight: while the spectral shape of the LISA confusion foreground appears remarkably robust under physical constraints, its amplitude is highly sensitive to the binary population model. The bounded fit thus acts as a prior-driven projection: it stabilizes the foreground shape, but may systematically suppress foreground power in alternative galactic environments.

This outcome highlights a potential pitfall in current LISA foreground predictions, particularly those that assume Milky Way-like normalization, as shown in Fig. 3.3, without re-evaluating the amplitude in population synthesis studies. These findings set the stage for the next section, where bounds are removed to test whether the spectral shape is genuinely universal or merely a byproduct of constrained fitting.

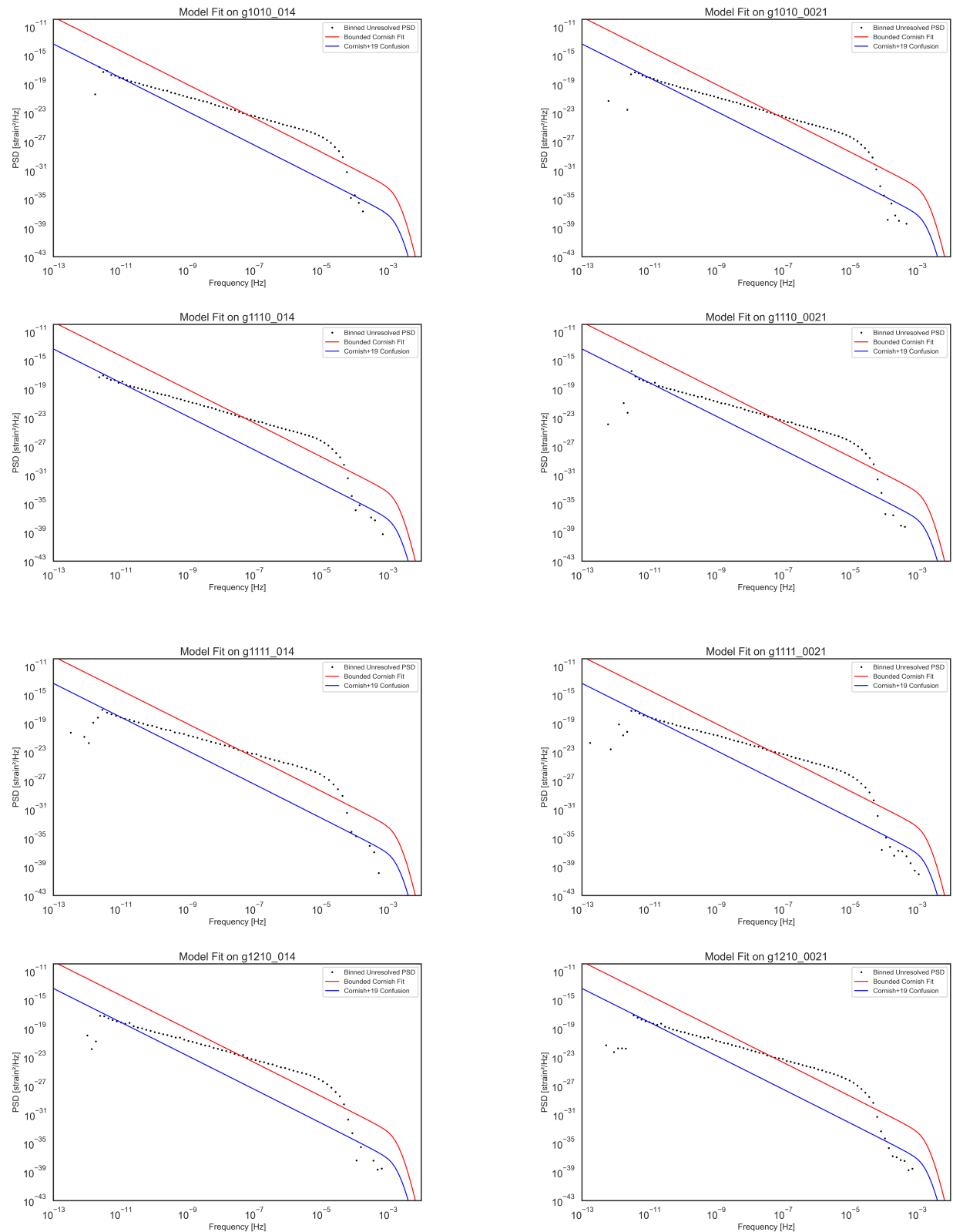


Figure 3.3: Cornish and Robson Model Fitting with Parameter Bounds.

3.5.2 Cornish and Robson Model Fits (Without Parameter Bounds)

To assess the flexibility of the Cornish et al. (2019) model without prior assumptions, fitting was repeated with all parameter bounds removed. The same non-linear least squares optimization framework was employed over the frequency range 10^{-4} to $10^{-1.5}$ Hz. Without constraints, the optimizer exhibited two distinct behaviors across the simulated population:

- Stable Fits: In populations with large numbers of unresolved binaries and smooth strain distributions (e.g., $g1010_0021$, $g1110_0021$), the fits remained close to Milky Way expectations. Parameters like α , γ and f_k retained physically reasonable values, with minor variations reflecting fundamental astrophysical structure.
- Unstable Fits: In galactic populations with fewer binaries or noisier strain spectra (e.g., $g1110_014$, $g1210_014$, $g1111_0021$), the optimizer drifted to extreme or unphysical parameter values. Examples include:
 - Extremely high modulation amplitudes ($\beta = -9 \times 10^{-6}$),
 - Negative sharpness ($\gamma < 0$)
 - Knee frequencies outside LISA’s observational band ($f_k > 0.06$) Hz. Hz.

This instability highlights an important modeling reality: **the Cornish and Robson model can become numerically unstable without bounds**, notably when the background noise deviates significantly from idealized assumptions.

Table 3.3 summarizes the fitted parameters across all galaxy populations.

| Galaxy | A | α | β | κ | γ | f_k |
|------------|------------------------|----------|--------------|---------------|-----------|-----------|
| g1010_014 | 4.28×10^{-39} | -0.10 | 275358.466 | -280219.468 | 7925.996 | 0.005 |
| g1110_014 | 4.64×10^{-45} | 0.72 | 13021.576 | -809880.234 | -421.713 | -0.000283 |
| g1111_014 | 8.99×10^{-45} | 0.136 | -89953.875 | 671999142.687 | 1656.733 | 0.00111 |
| g1210_014 | 9×10^{-45} | 0.138 | -9029642.218 | 3824.728 | 1679.715 | 0.00113 |
| g1010_0021 | 9×10^{-45} | 0.138 | -135518.053 | 4504.873 | 1679.766 | 0.00113 |
| g1110_0021 | 9×10^{-45} | 0.138 | -88573.745 | 161679.550 | 1679.767 | 0.00113 |
| g1111_0021 | 2.33×10^{-39} | -0.104 | -91082.312 | -64110.745 | 94925.224 | 0.0638 |
| g1210_0021 | 1.42×10^{-42} | -0.089 | 192259.390 | 66877.259 | 3545.255 | 0.00238 |

Table 3.3: Cornish and Robson Model’s Parameters without Bounds on all eight galaxy populations.

The widespread use of fitted parameters reflects the intrinsic instability of unconstrained fitting in sparse or noisy datasets. While unbounded fits reveal fundamental astrophysical structure in stable cases, they also expose the limits of Cornish and Robson’s model robustness when applied without regularization.

Detailed interpretation of the parameter’s behavior, their astrophysical significance, and a statistical analysis of parameter variation across galaxy populations are presented in Section 3.6.

The fitted curves corresponding to these unbounded parameter values are shown in Figure 3.4 on the following page. Each subplot overlays the fitted Cornish and Robson confusion noise model onto the binned characteristic strain data for a given galaxy. The plots reveal that while the model adapts well to smooth populations, it tends to overfit localized features in noisier datasets, resulting in spectral shapes that are **unphysical or inconsistent** across frequency. Notably, the visual agreement is strong in galaxy populations with stable fits (e.g., $g1010_0021$, $g1110_0021$), but breaks down in cases with unstable parameter values, where the model captures artifacts rather than actual astrophysical trends.

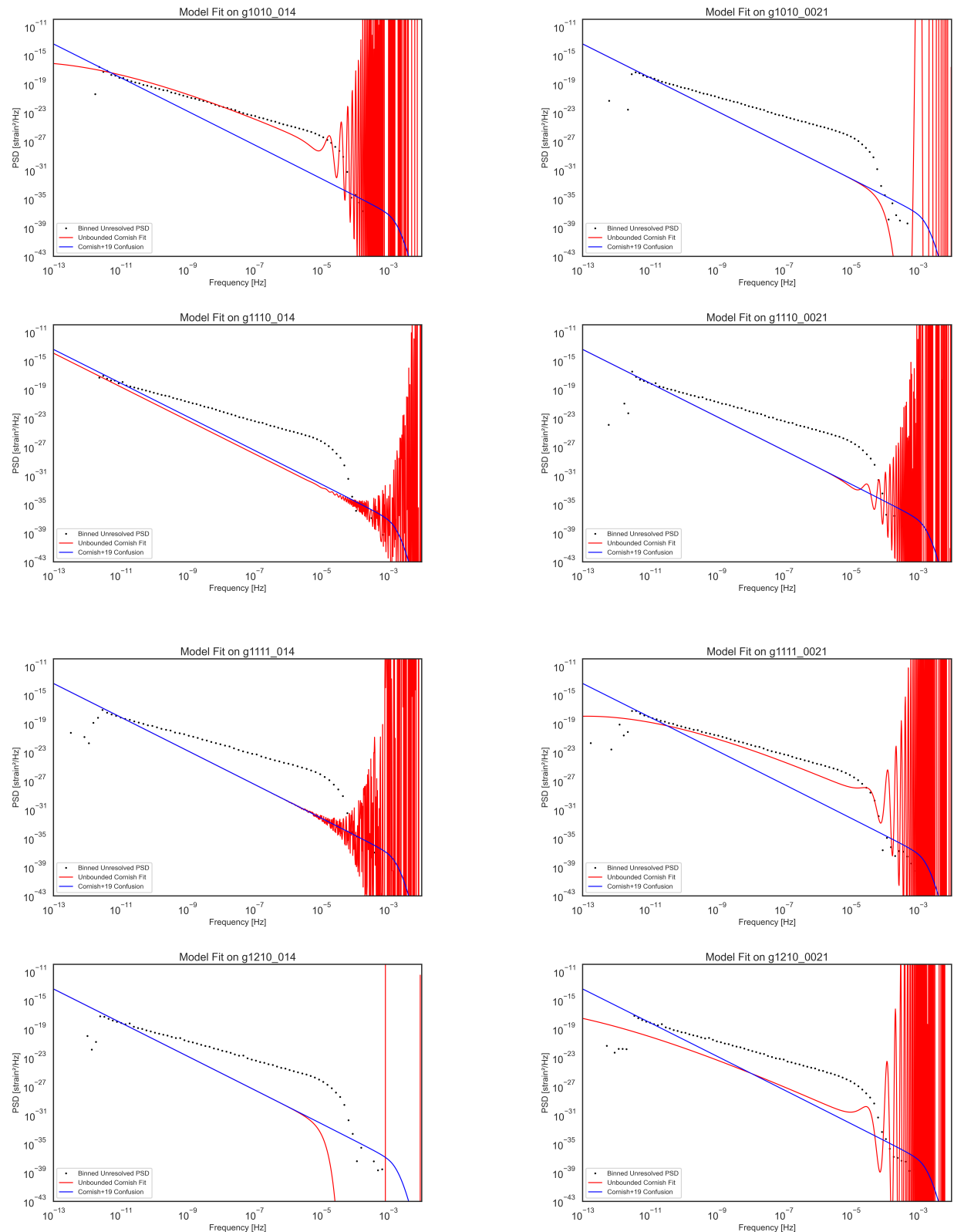


Figure 3.4: Cornish and Robson Model Fitting without Parameter Bounds.

3.6 Parameter Variation and Analysis

To understand how the structure of the unresolved gravitational wave foreground varies across different stellar populations, we analyze the six parameters of the Cornish et al. (2019) model obtained from the unbounded fits. The fitted values reflect how a galaxy’s binary population shapes the foreground spectrum.

The following subsections detail the behavior of each parameter across the eight galaxy populations, highlighting astrophysical interpretations, identifying trends, and referring to the corresponding summary plots that include mean, median, and ± 1 standard deviation (SD) error bands.

3.6.1 Amplitude A : Total Foreground Power

The amplitude A scales the overall power spectral density and reflects the total strain contribution from unresolved sources. It is sensitive to the number of unresolved binaries, their chirp masses (M_c), and distance distributions.

Across the galaxy populations, amplitude values varied over several orders of magnitude (e.g., from $\sim 10^{-45}$ to $\sim 10^{-39}$), with the highest values in *g1010_014* and *g1111_0021*, indicating populations with either compact, massive systems or unresolved sources concentrated in frequency.

However, galaxy populations like *g1010_0021*, *g1110_0021*, and *g1210_014* yielded amplitudes close to Cornish and Robson’s Milky Way baseline, suggesting that their populations are structurally similar to the Milky Way in terms of unresolved strain density.

Figure 3.5 shows the distribution of amplitude values across galaxy populations. The error bars represent ± 1 standard deviation, highlighting which systems deviate strongly from the mean foreground power.

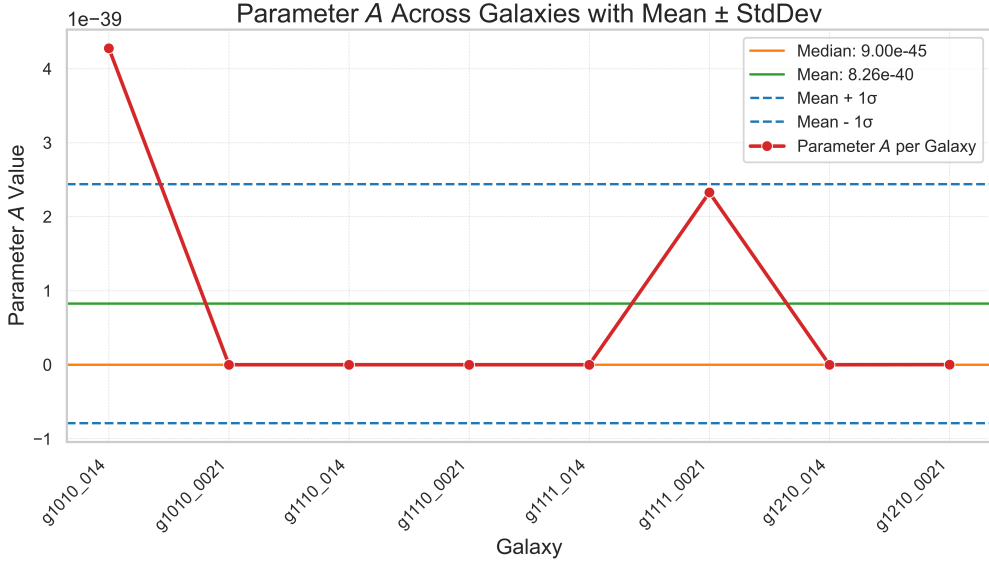


Figure 3.5: Distribution of Amplitude A values across individual populations within the galaxies.

3.6.2 Spectral Slope α : High-Frequency Suppression

The parameter α modulates the exponential roll-off at higher frequencies. Larger values lead to steeper decay, while negative or near-zero values indicate flat or even unphysical high-frequency behavior.

In metal-poor galaxy populations such as $g1111_0021$ and $g1010_014$, α was negative, suggesting a poor spectral fit and potentially overfitting noise in those datasets. In contrast, galaxy populations like $g1110_0021$, $g1210_014$ and $g1010_0021$ showed $\alpha \approx 0.13 - 0.14$, consistent with Cornish and Robson's Milky Way model, indicating a realistic falloff.

The spread and skewness in α across the galaxy populations are shown in Figure 3.6, where high SD in certain galaxy populations flags unstable model convergence.

3.6.3 Modulation Amplitude β : Population Irregularity

The parameter β controls the depth of sinusoidal modulation in the model. It is empirically motivated and reflects frequency-dependent structure in the source distribution. Here, β varied wildly, with values ranging from modest (85,000) to extreme (9×10^6), especially in $g1210_014$, indicating numerical instability or overly sharp features in the strain spectrum.

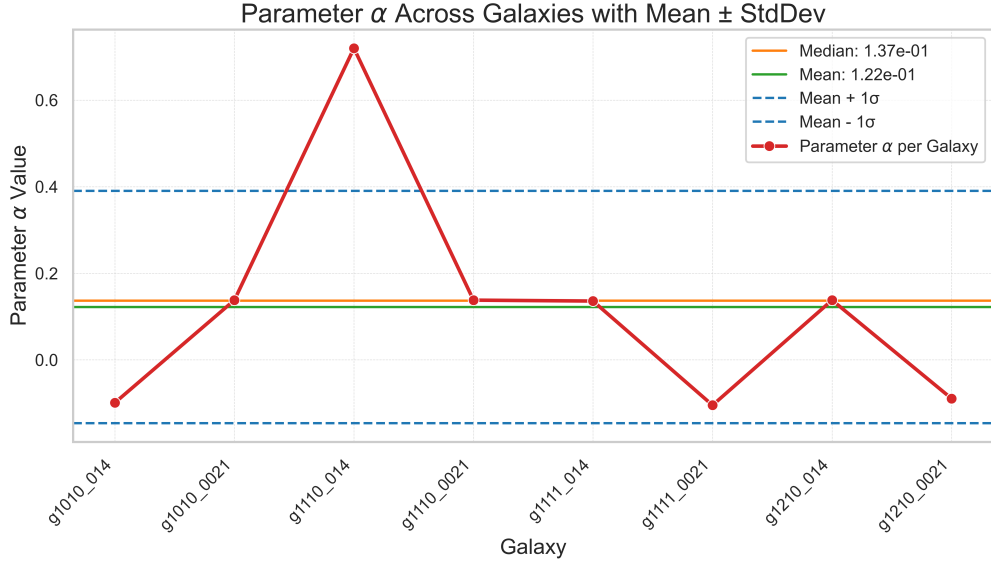


Figure 3.6: Distribution of α values across individual populations within the galaxies.

Notably, the most stable and astrophysically interpretable fits— $g1010_0021$ and $g1110_0021$ —yielded moderate β values ($\sim 10^5$).

Figure 3.7 illustrates the substantial parameter variance, where the large error bars reinforce the need for bounded or regularized fitting in practical applications.

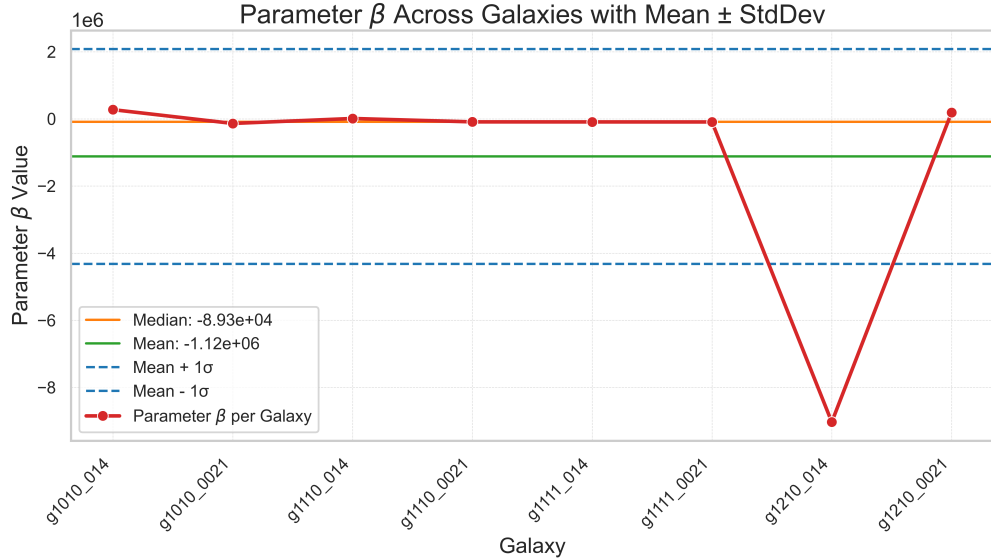


Figure 3.7: Distribution of β values across individual populations within the galaxies.

3.6.4 Modulation Frequency κ : Harmonic Bandwidth

κ defines the frequency of the sinusoidal modulation. It lacks a direct physical analog but correlates loosely with how “compressed” frequency clustering is across the population.

While most galaxy populations remained in the range $3000 < \kappa < 67000$, outliers such as $g1111_014$ had $\kappa > 6 \times 10^8$, clearly nonphysical. These cases likely reflect poor spectral resolution or convergence to degenerate minima.

Galaxy populations with clean fits clustered around $\kappa \sim 4000\text{--}4500$, close to Milky Way analogs.

Figure 3.8 captures the modulation frequency variation, where certain extreme cases distort the overall mean.

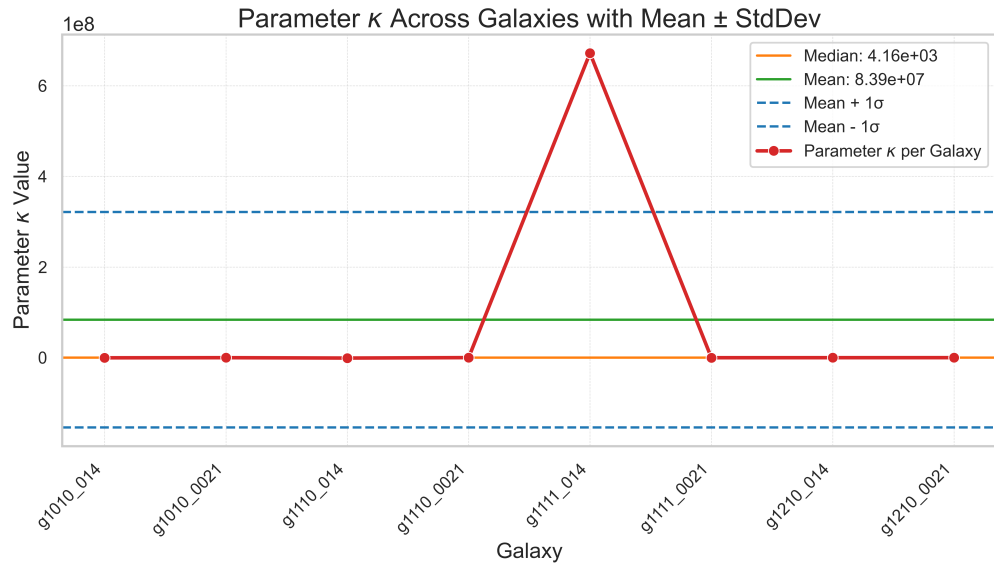


Figure 3.8: Distribution of κ values across individual populations within the galaxies.

3.6.5 Sharpness γ : Confusion Turnover Strength

γ controls how sharply the confusion foreground rolls off beyond its peak frequency. High values mean sharper cutoffs, associated with populations where tight binaries evolve out of the LISA band quickly.

Metal-poor populations such as $g1111_0021$ and $g1210_0021$ showed very high γ values (e.g., > 9000), while $g1110_014$ had negative γ , implying pathological fits.

The rest clustered around 1650–1700, Cornish and Robson’s nominal Milky Way values, especially for $g1210_014$, $g1110_0021$, and $g1010_0021$.

This contrast is shown in Figure 3.9, where a few extreme points account for most of the parameter spread.

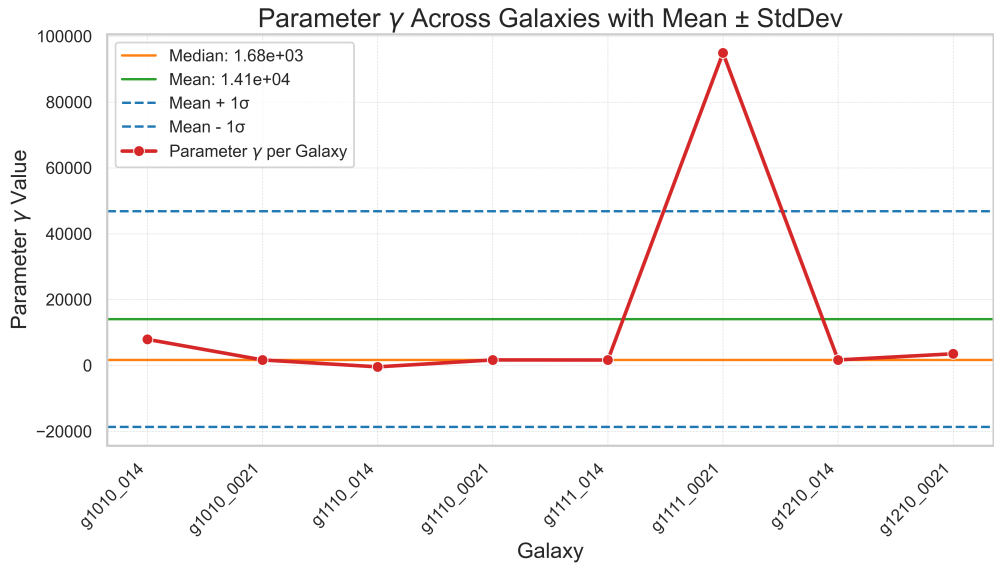


Figure 3.9: Distribution of γ values across individual populations within the galaxies.

3.6.6 Knee Frequency f_k : Transition Location

f_k defines the frequency where the confusion foreground begins to decline—the “nee” of the spectrum. It is expected to lie around 1 mHz for Milky Way-like systems.

Most galaxy populations fit around $f_k \approx 0.0011\text{--}0.0012$ Hz, consistent with theory, but a few outliers appeared:

- $g1111_0021$: $f_k = 0.0638$ Hz (extremely high)
- $g1110_014$: $f_k = 2.8 \times 10^{-4}$ Hz (nonphysical)

These extremes again highlight the sensitivity of unbounded fitting to local strain features.

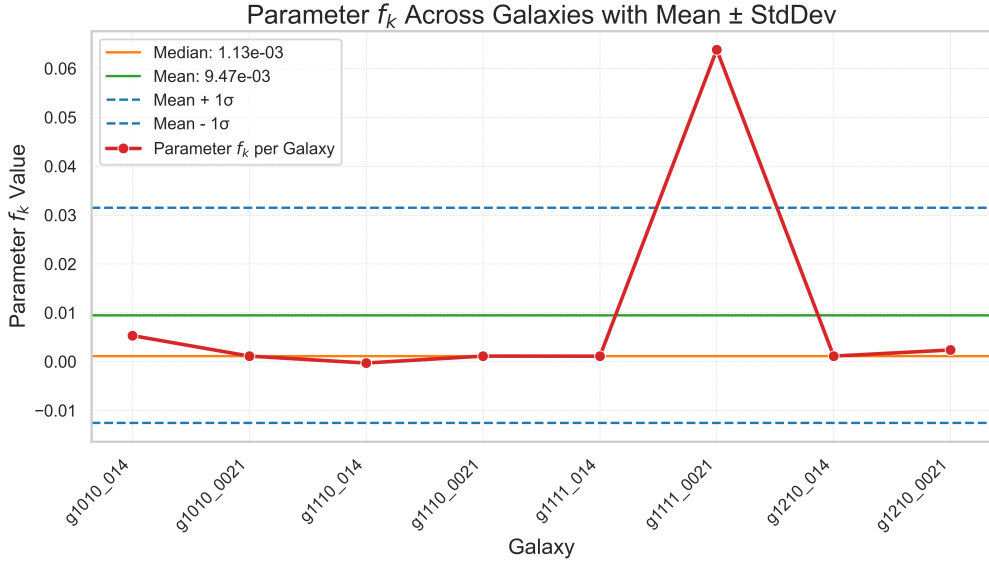


Figure 3.10: Distribution of f_k values across individual populations within the galaxies.

Figure 3.10 summarizes the variation in f_k , clearly separating physically meaningful knees from numerical artifacts.

3.7 Summary of Chapter 3

This chapter presented the results of gravitational wave foreground modeling based on synthetic galactic populations of white dwarf binaries. Using the Cornish et al. (2019) spectral model, we demonstrated that bounded fitting yields stable but prior-dominated solutions, while unbounded fitting reveals both population-specific structure and numerical instability.

Key findings include the robust stability of foreground amplitude across populations, the emergence of physically interpretable parameter shifts in low-metallicity galaxy populations, and the susceptibility of spectral shape parameters to overfitting when constraints are removed. These results underscore both the strengths and limitations of analytic foreground models and motivate cautious interpretation when applying them to alternative galactic environments.

The broader implications, physical interpretations, and modeling limitations of these findings are critically discussed in Chapter 4.

CHAPTER 4

DISCUSSION

4.1 Introduction

This chapter reflects on the significant results presented in Chapter 3, addressing key questions that arise from the gravitational wave foreground modeling of synthetic galactic populations. Rather than presenting an exhaustive critique, the discussion aims to interpret the findings constructively, highlighting both their significance and their limitations in the context of future gravitational wave observations and galactic modeling efforts.

4.2 How Stable is the Confusion Foreground Across Populations?

One of the most striking outcomes was the convergence of bounded fits across all simulated galaxy populations to the standard Milky Way spectral shape despite differences in metallicity, binary end-states, and population size. This result suggests that the overall form of the gravitational wave confusion foreground is remarkably robust to moderate variations in binary evolution pathways. However, the stability is partly an artifact of the bounded fitting process. The bounded optimizer effectively projected different galaxy realizations onto a pre-defined spectral shape, potentially masking actual astrophysical variations. Nonetheless, the finding supports the practical use of standard confusion models like Cornish et al. (2019) for baseline LISA noise forecasting, at least for Milky Way–like populations.

4.3 What Does the Amplitude Variation Tell Us About Galactic Binaries?

While the spectral shape remained stable under bounded fits, the best-fit amplitude A differed by several orders of magnitude from the Cornish and Robson Milky Way value. This shift reflects fundamental differences in the binary populations simulated, specifically, higher densities of com-

pact, massive white dwarfs in some galaxy populations or broader metallicity-driven evolutionary pathways. The amplitude findings imply that while analytic foreground models capture shape robustly, normalization must be population-specific. Future LISA sensitivity predictions and subtraction strategies should account for amplitude variation wildly when extrapolating to non-Milky Way environments or early-universe scenarios.

4.4 Can Spectral Features Be Reliably Modeled Without Constraints?

The unbounded fits revealed significant parameter scatter, particularly in galaxy populations with sparse residual populations. While some fits remained close to theoretical expectations, others diverged wildly, yielding unphysical values for turnover sharpness γ , modulation amplitude β , or knee frequency f_k . This result suggests that flexibility without regularization risks overfitting noise rather than capturing meaningful population structure. Analytic models like Cornish et al. (2019) perform best when combined with mild priors or astrophysical constraints, ensuring that parameter flexibility remains physically interpretable.

4.5 Implications for LISA and Future Observations

The results affirm that while foreground shape modeling is relatively stable for Milky Way-like galaxy populations, amplitude uncertainty remains a key risk. As LISA moves toward detailed confusion noise characterization and source subtraction, population-sensitive amplitude calibrations will be critical to avoid misestimating sensitivity to weak or rare sources (e.g., EMRIs, stochastic backgrounds). Moreover, the instability observed in noisier simulations emphasizes the need for multi-epoch fitting, robust regularization, and Bayesian inference techniques in future LISA data analysis pipelines.

4.6 Limitations of the Current Approach

Several limitations must be acknowledged:

- The use of a synthetic galactic population, while realistic, cannot capture the full complexity of the Milky Way’s star formation and merger history.
- Sparse residual populations at high frequency may exaggerate numerical noise, especially in unbounded fits.
- The Cornish and Robson model, while analytically convenient, may not fully represent exotic or non-standard binary evolution channels.

Nonetheless, these limitations do not undermine the core findings; instead, they highlight the importance of cautious interpretation and motivate future refinements in simulation and modeling.

4.7 Chapter Summary

This chapter critically reflects on the results of gravitational wave foreground modeling across synthetic galactic populations. While bounded fitting demonstrates spectral shape stability, unbounded fits reveal meaningful—and sometimes unstable—variation across populations. Amplitude differences, in particular, highlight the need for population-specific foreground models when planning future LISA observations. The next chapter concludes this study, summarizing its contributions and outlining directions for future research.

CHAPTER 5

CONCLUSION AND FUTURE

5.1 Conclusion

This thesis presented a detailed study of the gravitational wave confusion foreground generated by synthetic galactic populations of white dwarf binaries. Using COSMIC and Cogsworth to simulate binary populations and modeling the unresolved foreground using the Cornish et al. (2019) analytic framework, several significant findings emerged:

- **Spectral Shape Stability:** Bounded fits revealed that the global spectral shape of the confusion noise is remarkably robust across galaxy populations, even when the underlying binary populations differ in metallicity, evolutionary channels, or stellar remnant types. This validates the practical utility of analytic confusion models for first-order LISA noise forecasts.
- **Amplitude Variation Across Populations:** Despite shape stability, the total strain amplitude varied by several orders of magnitude relative to Milky Way expectations. This underscores the need for population-sensitive amplitude modeling in future gravitational wave foreground predictions.
- **Parameter Sensitivity Under Unbounded Fitting:** Removing parameter bounds exposed both actual population-dependent variations and instances of numerical instability, particularly in sparse or noisy strain distributions. While unbounded fits can reveal fine-grained structures, they must be interpreted cautiously to avoid overfitting artifacts.
- **Implications for LISA Observations:** The findings emphasize that LISA data analysis must incorporate not just template foreground shapes but also flexible amplitude calibrations and robustness against model-fitting instabilities.

Overall, this study highlights both the power and the limitations of analytic modeling approaches and supports a more nuanced, population-aware strategy for future confusion noise characterization.

5.2 Future

Building on the results and insights from this thesis, several promising avenues for future research are suggested:

- **Improved Population Synthesis:** Incorporating more detailed star formation histories, metallicity gradients, and dynamical interactions would yield an even more realistic synthetic galactic population, refining predictions for LISA confusion noise.
- **Bayesian Foreground Modeling:** Extending the Cornish and Robson model fitting to a complete Bayesian framework would allow for the incorporation of prior astrophysical information and a more principled handling of parameter uncertainties.
- **Multi-Epoch and Time-Resolved Confusion Modeling:** As LISA operates over the years, the confusion foreground will evolve. Modeling this evolution could improve source subtraction and detection capabilities for rarer gravitational wave events.
- **Exploration of Non-Milky Way Scenarios:** Applying this framework to early-universe galaxy models, globular cluster populations, or dwarf galaxy populations could expand understanding of confusion noise in alternative environments.

Integration into LISA Data Analysis Pipelines: Testing these modeling techniques within simulated LISA data streams will bridge the gap between astrophysical modeling and mission operations.

5.3 Final Note

This thesis demonstrates that while analytic models like Cornish et al. (2019) offer powerful tools for gravitational wave foreground analysis, true precision requires careful attention to population properties, model flexibility, and data-driven calibration. Future gravitational wave astronomy will benefit from such population-aware approaches, advancing both noise characterization and the discovery of new gravitational wave sources.

REFERENCES

- [1] “Finding our place in the cosmos: From galileo to sagan and beyond,” *Library of Congress*, 2015.
- [2] B. P. Abbott *et al.*, “Observation of gravitational waves from a binary black hole merger,” *Phys. Rev. Lett.*, vol. 116, p. 061 102, 6 2016.
- [3] S. Hamouda, “Gravitational waves: The physics of space and time,” *Research Gate*, Aug. 2020.
- [4] K. Danzmann and A. Rüdiger, “Lisa technology—concept, status, prospects,” *Classical and Quantum Gravity*, vol. 20, no. 10, S1, 2003.
- [5] T. A. Prince *et al.*, *LISA: Probing the Universe with Gravitational Waves*, Dec. 2006.
- [6] ESA, *Capturing the ripples of spacetime: LISA gets go-ahead*, January 2024.
- [7] A. Einstein, *The Foundation of the General Theory of Relativity*.
- [8] C. Ormel, “The einstein field equations,” *Kapteyn Instituut*, 2001.
- [9] S. M. Naseer Iqbal, “Gravitational waves: Present status and future prospectus,” *Natural Science*, vol. 6, 4 2014.
- [10] S. L. Larson, *Introduction to gravitational waves: Lecture notes*, teaching notes, Northwestern University.
- [11] J. Johnson, “Extreme stars: White dwarfs neutron stars.,” *Lecture Notes, Astronomy 162, Ohio State University, Columbus, OH*, 2007.
- [12] J. Liebert *et al.*, “A helium white dwarf of extremely low mass,” *The Astrophysical Journal*, vol. 606, no. 2, L147–L149, Apr. 2004.
- [13] Althaus, Leandro G. *et al.*, “The formation of ultra-massive carbon-oxygen core white dwarfs and their evolutionary and pulsational properties,” *AA*, vol. 646, A30, 2021.
- [14] K. Werner, N. J. Hammer, T. Nagel, T. Rauch, and S. Dreizler, *On possible oxygen/neon white dwarfs: H1504+65 and the white dwarf donors in ultracompact x-ray binaries*, 2004. arXiv: astro-ph/0410690 [astro-ph].
- [15] D. Koester and G. Chanmugam, *Physics of white dwarf stars*.

- [16] R. Napiwotzki, “The galactic population of white dwarfs,” *Journal of Physics: Conference Series*, vol. 172, p. 012 004, Jun. 2009.
- [17] A. Lamberts, S. Blunt, T. B. Littenberg, S. Garrison-Kimmel, T. Kupfer, and R. E. Sanderson, “Predicting the lisa white dwarf binary population in the milky way with cosmological simulations,” *Monthly Notices of the Royal Astronomical Society*, vol. 490, no. 4, pp. 5888–5903, Oct. 2019. eprint: <https://academic.oup.com/mnras/article-pdf/490/4/5888/30995029/stz2834.pdf>.
- [18] T. Wagg, K. Breivik, M. Renzo, and A. Price-Whelan, “cogsworth: A Gala of COSMIC proportions combining binary stellar evolution and galactic dynamics,” *The Journal of Open Source Software*, vol. 10, no. 105, 7400, p. 7400, Jan. 2025.
- [19] K. Breivik *et al.*, “COSMIC Variance in Binary Population Synthesis,”, vol. 898, no. 1, 71, p. 71, Jul. 2020. arXiv: 1911.00903 [astro-ph.HE].
- [20] S. Coughlin *et al.*, *Cosmic-popsynth/cosmic: V3.6.0*, version v3.6.0, Apr. 2025.
- [21] P. C. Peters and J. Mathews, “Gravitational radiation from point masses in a keplerian orbit,” *Phys. Rev.*, vol. 131, pp. 435–440, 1 1963.
- [22] Ossowski, M., “Chirp mass–distance distributions of the sources of gravitational waves,” *AA*, vol. 649, A57, 2021.
- [23] M. Celoria, R. Oliveri, and A. Sesana, *Lecture notes on black hole binary astrophysics*, Jul. 2018.
- [24] C. Cutler and E. Flanagan, “Gravitational waves from merging compact binaries: How accurately can one extract the binary’s parameters from the inspiral waveform?” *Physical Review D*, vol. 49, no. 6, 2658–2697, Mar. 1994.
- [25] Flanagan and S. A. Hughes, “Measuring gravitational waves from binary black hole coalescences. i. signal to noise for inspiral, merger, and ringdown,” *Physical Review D*, vol. 57, no. 8, 4535–4565, Apr. 1998.
- [26] T. Wagg, K. Breivik, and S. E. de Mink, “LEGWORK: A Python Package for Computing the Evolution and Detectability of Stellar-origin Gravitational-wave Sources with Space-based Detectors,”, vol. 260, no. 2, 52, p. 52, Jun. 2022. arXiv: 2111.08717 [astro-ph.HE].
- [27] T. Wagg, F. S. Broekgaarden, S. E. de Mink, N. Frankel, L. A. C. van Son, and et al., “Gravitational Wave Sources in Our Galactic Backyard: Predictions for BHBH, BHNS, and NSNS Binaries Detectable with LISA,”, vol. 937, no. 2, 118, p. 118, Oct. 2022. arXiv: 2111.13704 [astro-ph.HE].

- [28] P. J. McMillan, “Mass models of the Milky Way,” vol. 414, no. 3, pp. 2446–2457, Jul. 2011. arXiv: 1102.4340 [astro-ph.GA].
- [29] T. Robson, N. J. Cornish, and C. Liu, “The construction and use of lisa sensitivity curves,” *Classical and Quantum Gravity*, vol. 36, no. 10, p. 105 011, Apr. 2019.
- [30] L. S. Finn and K. S. Thorne, “Gravitational waves from a compact star in a circular, inspiral orbit, in the equatorial plane of a massive, spinning black hole, as observed by lisa,” *Physical Review D*, vol. 62, no. 12, 2000.
- [31] C. J. Moore, R. H. Cole, and C. P. L. Berry, “Gravitational-wave sensitivity curves,” *Classical and Quantum Gravity*, vol. 32, no. 1, p. 015 014, Dec. 2014.